SCHOOL OF GEOGRAPHICAL AND EARTH SCIENCES

UNDERGRADUATE DISSERTATION

Matriculation Number: 2115872B

Assessing Flood Risk for a Section of the Bintacan de Ilagan River, Isabela Province, Luzon Island, the Philippines.

2019 – 2020

University of Glasgow

School of Geographical and Earth Sciences

COVER SHEET FOR DISSERTATION

Declaration of Originality
(Bind this page into the dissertation following the title page)

Name: Alasdair Breasley

Matriculation Number: 2115872B

Course Name: Joint Honours Economics with Geography

Title of Dissertation: Assessing Flood Risk for a Section of the Bintacan de Ilagan River, Isabela Province, Luzon Island, the Philippines.

Number of words: 9978

Plagiarism is defined as the submission or presentation of work, in any form, which is not one's own, without acknowledgement of the sources. Plagiarism can also arise from one student copying another student's work or from inappropriate collaboration. The incorporation of material without formal and proper acknowledgement (even with no deliberate intention to cheat) can constitute plagiarism. With regard to dissertations, the rule is: if information or ideas are obtained from any source, that source must be acknowledged according to the appropriate convention in that discipline; and any direct quotation must be placed in quotation marks and the source cited immediately.

Plagiarism is considered to be an act of fraudulence and an offence against University discipline. Alleged plagiarism will be investigated and dealt with appropriately by the School and, if necessary, by the University authorities.

These statements are adapted from the University *Plagiarism Statement* (as reproduced in the *School Undergraduate Handbook*). It is your responsibility to ensure that you understand what plagiarism means, and how to avoid it. Please do not hesitate to ask class tutors or other academic staff if you want more advice in this respect.

Declaration: I am aware of the University's policy on plagiarism and I certify that this piece of work is my own, with all sources fully acknowledged.

Signed: 

Acknowledgements

I would like to thank the Philippines Department of Science and Technology and the University of the Philippines for allowing the use of LiDAR and bathymetric data for conducting this dissertation, collected as part of the Disaster Risk and Exposure Assessment for Mitigation (DREAM) Program. I would also like to thank my dissertation supervisors Trevor Hoey and Richard Williams for all their help.

Abstract

Hydraulic modelling is becoming an ever more important tool for assessing flood risk, with climate change increasing the frequency and intensity of flooding events globally. This dissertation focuses on a section of the Bintacan de Ilagan River in the Philippines – representative of a small ungauged topographically complex tropical upland catchment. Methods of modelling total flood inundation are reviewed in relation to their appropriateness for the study area. Sources of uncertainty in flood inundation modelling results are discussed and methods for quantifying and representing this uncertainty are reviewed in relation to their appropriateness for the study area. A hydraulic model is then created and uncertainties with model results are assessed and ranked quantitatively. Sources of uncertainty not analysed quantitatively in this dissertation are then discussed qualitatively. Results are analysed for a series of return period flood events and flood risk within the study area is assessed. General recommendations are then made in relation to the choice of methods used for modelling in catchments similar to the representative study area.

Contents

Chapter 1 – Introduction

1.1 – Global Flooding

Floodplains attract human settlement due to their fertile soils for agriculture, flat ground for construction, and ease of access to water. Flooding is one of the most common natural disasters experienced globally and causes causalities and loss of property on every inhabited continent. Flooding causes large scale destruction of property with over $40B of damage occurring annually worldwide (OECD., 2016). Approximately 250M people are affected by flooding annually (UN., 2013a) with 7,850 deaths caused on average each year (UN., 2015).

Flooding is set to become an even larger problem in the future due to climate change. The magnitude and frequency of extreme rainfall events, such as typhoons, are increasing due to climate change (Arnell & Gosling., 2016; Hirabayashi et al., 2013; Richardson et al., 2011). This increase is causing a corresponding increase in frequency and magnitude of flooding events globally (Arnell & Gosling., 2016; Hirabayashi et al., 2013), with average annual damages incurred steadily increasing over time (OECD., 2016). The number of people living on floodplains is also increasing rapidly (OECD., 2016) and this will lead to more frequent and more disastrous flood events (Hirabayashi et al., 2013).

1.2 – Flooding in the Philippines

In the Philippines especially, flooding poses a significant threat to human life and property. The Philippines experiences the fourth most natural disasters of any country in the world with the majority of these disasters being flood and storm events (UN., 2015). The country is hit by multiple typhoons each year which have historically caused considerable damage from the subsequent flooding. Notable typhoons in recent years include Super Typhoon Yolanda 2013 which caused $2.2B worth of damage and killed 6300 people (del Rosario., 2014; UN., 2013b), Super Typhoon Glenda 2014 which caused $885M worth of damage and killed 106 people (Ramos., 2014) and Super Typhoon Ompong 2018 which caused $627M worth of damage and killed 127 people (Jalad., 2018).

Flooding is set to become an even larger problem in the Philippines due to climate change increasing the frequency and intensity of typhoons. Due to the Philippines location in South East Asia it is within the area predicted to have the greatest increase of flood risk due to climate change as a result of changing El Niño Southern Oscillation conditions and seasonal rainfall patterns (Alfieri et al., 2017). The Philippines is therefore one of the most vulnerable countries in the world to the impacts of climate change and is predicted to have increased overall river flow, variability of flow and peak river flow – increasing flood risk in the country (Tolentino et al., 2016). The proportionally largest increase in peak river flow prediction is found on Luzon Island where the study area is located. Despite this the number of people living on floodplains in the country is steadily increasing e.g. the Cagayan River on Luzon Island sees a 1-2% increase in population within the floodplain annually (Balderama et al., 2017). The increasing intensity of rainfall events and growing number of people living on floodplains will inevitably increase flood risk in the Philippines in the future.

1.3 – Flood Modelling

Flood modelling is an important tool as it can predict the extent and depth of flood inundation and can be used to assess flood risk and potential damage caused by flooding. Flood modelling is a key part of the process for flood forecasting to issue flood warnings and raise public awareness. It can be used in the design of flood defence infrastructure and guide appropriate property development and planning. The importance of flood modelling is only going to become greater in the future, due to climate change and the increasing intensity and frequency of extreme rainfall events combined with rapidly increasing population on floodplains (Arnell & Gosling., 2016; Hirabayashi et al., 2013; OECD., 2016; Richardson et al., 2011).

1.4 – Gap in the Literature

The gap in the literature this dissertation aims to fill is a locational gap. National flood risk mapping has been undertaken by the University of the Philippines as part of the Disaster Risk and Exposure Assessment for Mitigation (DREAM) Program. This mapping has focused on all the main rivers within the Philippines and 5, 25 and 100-year flood inundation maps have been produced for these rivers (e.g. Paringit & Floresca., 2017). The Bintacan de Ilagan River however was not included in the flood risk mapping undertaken. No flood risk mapping for the area currently exists and this is problematic

as there is a significant risk of flooding, with the town of Rang-Ayan having had the main road bridge, two weirs/foot bridges and ~10 houses destroyed in a flood event caused by Super Typhoon Lawin in 2016 (Dingle et al., 2019). Flood risk mapping of this area would fill the locational gap in the literature for an otherwise well covered region.

1.5 - Aim

The aim of this dissertation is to assess flood risk on a section of the Bintacan de Ilagan River in Isabella Province, the Philippines. This was planned to be achieved through the use of computer modelling to simulate possible flood events and assess the risk the Bintacan River poses to the surrounding area.

1.6 – Objectives

The following series of objectives were developed to achieve this aim:

- To create a hydraulic model to simulate possible flood events and calibrate the model using remote sensing data.
- To perform sensitivity analysis on the model to determine which model variables have the largest impact on total flood inundation and to help understand the uncertainties associated with model results.
- To perform hydrological sensitivity analysis on the model to determine what affects changes in input hydrology would have upon total flood inundation and to help understand the uncertainties associated with model results.
- To generate production runs for 5, 10, 25, 50 and 100-year flood events and create flood inundation maps for these events.
- To evaluate flood risk within the study area using these flood inundation maps.

1.7 Dissertation Structure

This dissertation will firstly consider the relevant literature and theory in the *Literature Review* – assessing the different methods used in flood inundation modelling, discussing sources of uncertainty in flood inundation modelling results and assessing how these sources of uncertainty are quantified and represented. Secondly there will be a *Study Area* section detailing the characteristics of the study area. Then the *Methodology* will provide an explanation and justification of the methods used in relation to the study area and literature. The findings from these methods will then be recorded in the *Results* section followed by the *Discussion* which will include interpretation and analysis of results. Finally, the *Conclusion* will summarise the findings of this dissertation.

Chapter 2 – Literature Review

2.1 Background

The aim of this literature review is to assess different methods of flood inundation modelling, to determine sources of uncertainty in flood inundation modelling results and to assess how these sources of uncertainty are quantified and represented.

2.1.1 Flooding

A flood is defined as the raising and overflowing of a body of water onto normally dry land (Merriam-Webster., 2019). Flood hazard is defined as the magnitude and probability of a flood occurring and flood risk is defined as the product of flood hazard and the possible consequences (Wolfgang., 2005). Floods cause the loss of life and destruction of property on every inhabited continent with over $40B of damage dealt annually worldwide (OECD., 2016) and 7,850 deaths caused on average each year (UN., 2015). With global warming causing an increase in the frequency and magnitude of extreme rainfall events, and the population living on floodplains constantly growing, global flood risk is steadily increasing (Arnell & Gosling., 2016; Hirabayashi et al., 2013; OECD., 2016; Richardson et al., 2011). Flood inundation modelling can predict the extent and depth of flood inundation and is therefore becoming increasingly important as a way to assess flood risk and potential damage caused by flooding.

2.2 – Review of Flood Modelling Methods

In a review of flood inundation modelling Teng et al., 2017 splits the types of methods used into three categories: Empirical Methods, Hydrodynamic Models and Simple Conceptual Models.

2.2.1 Empirical Methods

Empirical methods involve using real world observations to understand how previous flood events occurred, including the use of measurements, remote sensing, and statistical models to collect, process and analyse flood related data. However, despite these observations being based on reality they are only a limited representation and have underlying assumptions and uncertainties, and should be treated as model results (Teng et al., 2017). Results from these methods are widely used as inputs for other types of methods, for calibration and validation (Paiva et al., 2013a; Paiva et al., 2013b;

Zischg., 2018). For example remote sensing has been widely used to validate and calibrate flood inundation models (Bates., 2012; Horrit., 2006; Pappenberger et al., 2007; Schumann et al., 2007; Schumann et al., 2009; Schumann et al., 2015; Smith., 1997) and LiDAR data used as an input for hydraulic models (Cobby et al., 2001; Cook & Merwade., 2009; Costabile et al., 2015; Fewtrell et al., 2011; Marks & Bates., 2000).

Advantages

Empirical methods are considered to be robust and accurate and are the most straightforward approach to retrieve information about flood events (Teng et al., 2017). Recent improvements in remote sensing have greatly increased the resolution and availability of data (Archer et al., 2018; Dottori et al., 2013; Sun et al., 2015), however the accuracy of data collected does depend on the acquisition and processing techniques used for different collection methods.

Disadvantages

Empirical methods only give a snapshot of the past and therefore wisdom of hindsight is a clear limitation as they cannot directly make predictions about the future. Model variables cannot be altered to make predictions about possible scenarios as there is no direct link to the hydrology (Teng et al., 2017). Empirical methods are also subject to engineering limitations e.g. in the creation of sensors, environmental limitations e.g. weather conditions preventing data collection, and processing limitations e.g. processing methods can alter results and introduce errors (Teng et al., 2017).

2.2.2 Hydrodynamic Models

Hydrodynamic models simulate the movement of water computationally by using equations that govern the motion of fluids, with different levels of complexity (Teng et al., 2017). These models are run in either steady state, where hydrological inputs are constant over time (e.g. Bradbrook et al., 2004; Cook & Merwade., 2009; Vora., et al, 2018), or in unsteady state where hydrological input changes over time (e.g. Ahmadisharaf et al., 2018; Bates & De Roo., 2000; Singh & Goyal., 2017; Skinner et al., 2015).

Advantages

Hydrodynamic models can be directly linked to hydrological models to provide flood risk mapping, flood forecasting and scenario analysis (Teng et al., 2017). Model inputs and variables can be altered to simulate different possible scenarios and can be used to investigate changes in input hydrology, floodplain conditions and topography. They can also quantify the extent, timing and duration of inundation with high accuracy (Neelz & Pender., 2013).

Disadvantages

Hydrodynamic models are computationally intensive and have significant data requirements to be used effectively (Teng et al., 2017). More complex hydrodynamic models cannot be used to model large scale catchments (>2000km^2) or used in probabilistic approaches requiring many model runs due to prohibitively long model run times (Neelz & Pender., 2013).

Types of Hydrodynamic Models

There are several types of hydrodynamic model which can be grouped into 1D, 2D and 3D models depending on their spatial representation of flow and the complexity of the equations they solve.

2.2.2.1 1D Models

1D models use the simplest representation of flow, treating flow as one-dimensional along the river centre line (Brunner., 2016; DHI., 2003; Jacobs., 2019). They can be used to model both in-channel flow and floodplain flow, with floodplain flow being treated as part of the in-channel flow – moving parallel to the river channel. In both cases water levels and flow are calculated using a series of cross-sections where the one-dimensional Saint-Venant equations (Figure. 2.2.2.1.) are solved by ensuring conservation of mass and momentum between cross-sections. 1D models make several assumptions however including the one-dimensionality of flow, uniformity of velocity and horizontality of water level across the cross-sections (Tayefi et al., 2007).

$$Conservation\ of\ mass \quad \frac{\partial Q}{\partial x} + \frac{\partial A}{\partial t} = 0$$

$$Conservation\ of\ momentum \quad \frac{1}{A}\frac{\partial Q}{\partial t} + \frac{1}{A}\frac{\partial (\frac{Q^2}{A})}{\partial x} + g\frac{\partial h}{\partial x} - g(S_0 - S_f) = 0$$

Figure. 2.2.2.1. *A box detailing the one-dimensional Saint-Venant equations which govern the conservation of mass and conservation of momentum for water in one dimension. Q is the flow discharge (Q = uA, where u is the cross-sectional averaged velocity and A is the cross-section area), t represents time, h is the water depth, g is the gravitational constant, S_f is the friction slope and S_0 is the channel bed slope. These one-dimensional equations are a simplification of the two-dimensional Saint-Venant equations (two-dimensional shallow water equations). These equations have no analytical solution but can be solved using numerical techniques. The solutions give estimates of Q and h for every cross section at each time step (Teng et al., 2017).*

Advantages

The main advantage of 1D models is that they are computationally efficient and have faster model run times than other types of hydrodynamic models (Teng et al., 2017). It is well acknowledged that in-channel flows may be satisfactorily described by 1D models (Tayefi et al., 2007) and in the absence of detailed topographic data 1D models can sometimes perform as well as 2D models for predicting flood inundation extent (Horritt & Bates., 2002).

Disadvantages

1D models have a number of disadvantages due to their model structure and assumptions being conceptually problematic when applied to overbank flows (Costabile et al., 2015; Horritt & Bates., 2002; Tayefi et al., 2007). They cannot simulate lateral diffusion of the flood wave, do not represent topography as a continuous surface, and the choice of cross-section location and orientation is subjective and affects flood inundation area (Cook & Merwade., 2009; Teng et al., 2017). 1D models cannot effectively predict flood inundation when there are significant 2D effects on flow e.g. in topographically complex floodplains (Samuels., 1990; Bates & Anderson., 1993; Tayefi et al., 2007).

2.2.2.2 2D Models

2D models represent flow in two dimensions and assume that the third dimension (water depth) is shallow in comparison to the other dimensions (DHI., 2012; Jacobs., 2019; Roberts et al., 2010). 2D models do not represent vertical movement within the water. These models use topographic data such as Digital Elevation Models (DEMs) as inputs and represent topography as a continuous surface. Flood inundation area, depth and velocity are calculated using the two-dimensional Saint-Venant equations (Figure. 2.2.2.2.) which ensure that the conservation of mass and momentum across the two-dimensional plain.

$$Conservation\ of\ mass \quad \frac{\partial h}{\partial t} + \frac{\partial (hv)}{\partial x} + \frac{\partial (hv)}{\partial y} = 0$$

$$Conservation\ of\ momentum \quad \frac{\partial (hu)}{\partial t} + \frac{\partial}{\partial x}\left(hu^2 + \frac{1}{2}gh^2\right) + \frac{\partial (huv)}{\partial y} = 0$$

$$\frac{\partial (hv)}{\partial t} + \frac{\partial (huv)}{\partial x} + \frac{\partial}{\partial y}\left(hv^2 + \frac{1}{2}gh^2\right) = 0$$

Figure. 2.2.2.2. *A box detailing the two-dimensional Saint-Venant equations which govern the conservation of mass and momentum of water in two dimensions, assuming the third dimension is shallow in comparison to the other two dimensions. The two-dimensional Saint-Venant equations are found by depth averaging the Navier-Stokes equations which themselves govern the motion of viscous fluid substances. x and y are the two spatial dimensions, and the 2D vector (u, v) is the horizontal velocity averaged across the vertical column. The solution of these equations gives estimates of u, v and h over space and time. As with the one-dimensional Saint-Venant equations, the two-dimensional Saint-Venant equations have no analytical solution and many numerical schemes have been developed for algebraic approximation (Teng et al., 2017).*

Advantages

2D models have several advantages over 1D models, with their accuracy when modelling floodplain flow being the main advantage. Studies (Neelz & Pender., 2010; Neelz & Pender., 2013) have found that 2D models are capable of predicting velocity, flood extent and water levels with high accuracy and have demonstrated their benefits over 1D models for predicting flood inundation (Cobby et al., 2002; Cook & Merwade., 2009; Horrit & Bates., 2002; Horrit et al., 2006; Tayefi et al., 2007). Also, for some studies flow velocity is important, such as in steep upland areas and flood wall breaches (Moel et al., 2009; Qi & Altinakar., 2011), and velocity is required for flood hazard

assessment studies (Ernst et al., 2010; Balica et al., 2013) making 2D modelling necessary.

Disadvantages

The main disadvantage of 2D models is that they are computationally intensive. 2D models are generally considered unviable for areas >1000km^2 and for probabilistic methods requiring large numbers of model runs due to prohibitively long run times (Neelz & Pender., 2013; Teng et al., 2017). 2D models become more computationally intensive as DEM grid size is decreased due to the Courant-Friedrichs-Lewy stability condition requiring smaller timesteps (Courant et al., 1967; Neal et al., 2011; Neelz & Pender., 2010; Neelz & Pender 2013; Schubert et al., 2008). Due to their two-dimensional representation of flow 2D models cannot reproduce the details of vertical flow processes effectively (Soares-Frazao et al., 2008; Guinot., 2012) and are therefore not appropriate for modelling dam breaks, tsunamis, or embankment breaches (Teng et al., 2017).

2.2.2.3 3D Models

3D models represent flow in three dimensions and were developed to allow representation of vertical features and flows (Monaghan., 1994; Ye & McCorquodale., 1998). Some 3D models solve horizontal flow using the two-dimensional Saint-Venant equations with a quasi-3D extension to model velocity in vertical layers (Casulli & Stering., 1998) and others use the three-dimensional Navier-Stokes equations (Figure. 2.2.2.3.) to model flow (Cleary & Prakash, 2004; Monaghan., 1994; Prakash et al., 2014; Vacondio et al., 2011).

$$Conservation\ of\ momentum \quad \frac{\partial u}{\partial t} + u \cdot \nabla u + \frac{1}{\rho}\nabla p = g + \mu \nabla \cdot \nabla u$$

$$Incompressibility\ condition \quad \nabla \cdot u = 0$$

Figure. 2.2.2.3. *A box detailing the three-dimensional Navier-Stokes equations which govern the motion of viscous fluid substances. u is velocity, ρ is the fluid density, p is pressure, g is the gravitational constant and μ is the kinematic viscosity. The first equation comes from applying Newton's equation F = ma to fluid motion. The second equation is based on the assumption that the material density is constant within a fluid (Teng et al., 2017).*

Advantages

3D models have advantages over 2D models due to their representation of vertical flow. 2D models cannot reproduce the details of vertical flow processes which 3D models can (Soares-Frazao et al., 2008; Guinot., 2012). 3D models are therefore more accurate for modelling situations where vertical flow is a significant factor, such as dam breaks, tsunamis, embankment breaches or flow in road junctions (Cleary & Prakash., 2004; Mignot et al., 2006; Teng et al., 2017).

Disadvantages

The main disadvantage of 3D models is that they are extremely computationally intensive and have longer model run times than other hydrodynamic models, with modelling at the reach scale (>1km) recently considered unviable (Teng et al., 2017). 3D models have also suffered from problems of accurately representing free surface flows, high-order turbulence and a transient flood shoreline (Teng et al., 2017).

2.2.2.4 1D/2D Linked Models

1D/2D linked models link together both a 1D model and a 2D model and run them simultaneously. Usually the river channel will be modelled in 1D and the floodplain modelled in 2D. As the models are run together water is dynamically pushed between the 1D and 2D models and vice versa through link lines which act as a boundary between the models with different types of links used by different developers e.g. lateral link, longitudinal link and vertical link (Neelz & Pender., 2009).

Advantages

1D/2D linked models utilise the advantages of both 1D and 2D models. Most importantly 1D models' ability to effectively model in-channel flow (Tayefi et al., 2007) and 2D models' ability to effectively model floodplain flow (Neelz & Pender., 2009; Neelz & Pender., 2010; Neelz & Pender., 2013; Tayefi et al., 2007). It has been found that a linked 1D/2D approach, modelling the channel in 1D and the floodplain in 2D, provides the best outcome for floodplains with complex topography especially in upland areas (Tayefi et al., 2007).

Disadvantages

1D/2D models do have disadvantages, with the choice of linkage technique used altering results due to different volumes of water being moved between the 1D and 2D

models (Neelz & Pender., 2013). Different software packages use different linkage techniques and therefore results vary between packages e.g. predictions of velocities in urban areas vary significantly between packages (Neelz & Pender., 2013).

2.2.3 Simple Conceptual Models

Simple conceptual models use simplified representations of physics as opposed to the 'full physics' used in hydrodynamic models (Hunter et al., 2008; Neelz and Pender., 2010; Neelz and Pender., 2013). These simplified models use a 2D representation of flow but do not solve the 2D flow equations. They do not involve any simulation of the physical process of inundation and are based on simplified hydraulic concepts (Teng et al., 2017). For example, the RFSM method (L'homme et al., 2008), the HAND method (Nobre et al., 2011) and Flood Modeller FAST (Jacobs., 2019).

Advantages

The main advantage of simple conceptual models is that they are computationally efficient, with model run times often orders of magnitude faster than hydrodynamic models. Therefore, they are good for large scale applications (>2000km^2) (Teng et al., 2015) and for probabilistic flood risk assessment involving large numbers of model runs (Teng et al., 2017). In appropriate situations, with non-topographically complex floodplains, simple conceptual models can perform as well as hydrodynamic models when predicting inundation extent and depth (Afshari., 2018; Horritt & Bates., 2001a; Horritt & Bates., 2002; Hunter et al., 2008; Neelz & Pender., 2010; Neelz & Pender., 2013). Simple conceptual models are even fast enough to be appropriate for on demand online flood inundation modelling (McGrath., 2018).

Disadvantages

Simple conceptual models have considerable limitations, especially where dynamic effects and momentum conservation are important, due to their lack of representation of flow dynamics (Neelz & Pender., 2013). In topographically complex floodplains and hydraulically complex conditions simple conceptual models struggle to produce accurate results (Afshari., 2018; Teng et al., 2017). Most simple conceptual models do not give information on the propagation of the flood wave and flow velocity and are ineffective for studies which use these to assess flood hazard (e.g. Jonkman et al., 2008; Gomez-Valentin et al., 2009; Gomez et al., 2011; Xia et al., 2011; Russo et al., 2013).

2.3 – Uncertainty

Analysis of the uncertainties associated with model results is a key part of flood inundation modelling. Sources of uncertainty need to be identified, uncertainty from different sources needs to be quantified (or at least ranked qualitatively) and uncertainty needs to be communicated effectively (Beven et al., 2015; Dottori et al., 2013; Teng et al., 2017).

2.3.1 Sources of Uncertainty in Flood Inundation Modelling

There are many sources of uncertainty present in flood inundation modelling. Different sources of uncertainty can be determined by looking at model processes (Beven et al., 2015; Dottori et al., 2013). The main sources of uncertainty include: choice of model structure (Apel et al., 2009; Pappenberger et al., 2006; Renard et al., 2010; Willis et al., 2019), model parameters (Bates et al., 2004; Pappenberger et al., 2005, Romanowicz & Beven., 2003), model inputs (Abily et al., 2016; Pappenberger et al., 2008; Savage et al., 2016a; Merz & Thieken, 2005; Renard et al., 2010; Warmink et al., 2010; Beven et al., 2011.), changes in floodplain characteristics (Beven., 2010), changes in river morphology over time (Pender., 2016; Wong., 2015) and change in climatic conditions (Hirabayashi et al, 2013; Neal et al., 2013). Uncertainties from the choice of model structure (underlying equations and numerical methods) are difficult to quantify (Gupta et al., 2012) with uncertainties arising from the level of physical representation chosen (1D, 2D, etc.) having a significant effect on model results (Apel et al., 2009; Cook & Merade., 2009; Costabile et al., 2015; Horritt & Bates., 2002a; Tayefi et al., 2007; Willis et al., 2019). Uncertainties with model parameters are easier to quantify with the majority of studies focussing on floodplain roughness (Dung et al., 2011; Hall et al., 2005; Mason et al., 2003; Pappenberger et al., 2005; Pappenberger et al., 2007; Pappenberger et al., 2008). Uncertainties from model inputs include uncertainties with input hydrology, uncertainties with input topographic data and DEM grid size and uncertainties with input bathymetry (Abily et al., 2016; Bates et al., 1998; Bates et al., 2002; Beven et al., 2011; Merz & Thieken, 2005; Morgan et al., 2016; Pappenberger et al., 2008; Renard et al., 2010; Savage et al., 2016b; Tsubaki et al., 2013; Warmink et al., 2010; Yu and Lane, 2006). Also, there can be significant uncertainty in model validation and calibration data (e.g. satellite data) (Stephens et al., 2012).

2.3.2 Quantifying Uncertainty in Flood Inundation Modelling

Methods for quantifying uncertainty in model results are generally referred to as 'sensitivity analysis' (Hall et al., 2005). Sensitivity analysis can be used to quantify and rank the contribution of uncertainty in different variables to model results. There are two main types of sensitivity analysis: local sensitivity analysis and global sensitivity analysis (Savage., 2016a).

Local sensitivity analysis entails varying model parameters and inputs one at a time by a small amount around some fixed point and measuring the effect on model outputs (e.g. Tsubaki & Kawahara., 2013). The fixed point is often an estimate of the optimal parameters to represent reality (Savage., 2016a). Local sensitivity analysis is appropriate where models are computationally intensive and probabilistic sensitivity analysis would take a prohibitively long time (Neelz & Pender., 2013) and when dealing with complex models with too many variables to perform global sensitivity analysis.

Global sensitivity analysis entails varying all parameters simultaneously, typically using a sampling-based approach, and then assessing the effects of both individual variables and interactions between variables (e.g. Abily et al., 2016; Mara et al., 2015; Pappenberger et al., 2008). There are two commonly used global sensitivity analysis methods in flood modelling, Bayesian methods and General Likelihood Uncertainty Estimation (GLUE) methods (Beven & Binley., 1992; Beven & Binley., 2013). Bayesian methods use formal probability distributions and likelihood measures (e.g. Hall et al., 2011; Lui & Merwade., 2018) whereas GLUE methods use less formal pseudo-likelihood measures (Stephens & Bates., 2015). Nevertheless, the GLUE method has been widely used in flood inundation modelling (e.g. Aronica et al., 2002; Bates et al., 2004; Jung & Merwade., 2012; Romanowicz & Beven., 2003; Romanowicz et al., 2006; Sanyal et al., 2014; Yu et al., 2015).

2.3.3 Sensitivity Analysis Results from the Literature

2.3.3.1 Floodplain Roughness

Studies looking at the effects of altering floodplain roughness (Manning's n) values have found that increasing floodplain roughness generally increases total flood inundation area (Apel et al., 2009; Bates et al., 2004; Dung et al., 2011; Hall et al., 2005; Mason et al., 2003; Merwade et al., 2008; Pappenberger et al., 2005; Pappenberger et al., 2007; Pappenberger et al., 2008; Romanowicz & Beven., 2003). This is due to the increased friction slowing waters movement through the model, increasing the maximum volume of water within the model and increasing flood inundation.

2.3.3.2 Model Timestep

2D models require a choice of model timestep to be made which is usually related to the Courant-Friedrichs-Lewy condition (Courant et al., 1967; Neelz & Pender., 2013; Teng el al., 2017). Models generally have to have a timestep of less than 1/2 of the DEM resolution (m) to maintain model stability (CH2M, 2009). The choice of timestep is subjective however and can introduce uncertainty.

2.3.3.3 DEM Resolution

Studies looking at the effects of resolution of topographic data and altering DEM resolution (grid size) have found that lower resolution input topographic data, or resampling a DEM to a coarser resolution, generally increases total flood inundation area (Bates et al., 1998; Cook & Merwade., 2009; Horritt and Bates, 2001b; Yu and Lane, 2006; Savage et al., 2016a; Savage et al., 2016b). This is often due to the smoothing out of sub-grid topography allowing water to spread more easily (Dottori et al., 2013; Savage et al., 2016b).

2.3.3.4 Input Hydrology

Uncertainty in the input hydrology can have a significant effect on flood inundation results (Beven et al., 2011; Merz & Thieken., 2005; Pappenberger et al., 2006; Pappenberger et al., 2008; Renard et al., 2010., Savage et al., 2016a) with higher intensity events and larger peak flow values on the input hydrograph producing larger flood inundation areas. Input hydrology is also generally estimated using rating curves based upon previous high flow events but there are significant uncertainties associated with these curves (Pelletier., 1988).

2.3.4 Representing Uncertainty in Flood Modelling Results

The effective communication of results from uncertainty analysis is crucial in flood inundation modelling (Beven et al., 2015; Dottori et al., 2013). Deterministic flood maps do not communicate the uncertainties associates with them and could lead to false confidence, with the high-resolution outputs not necessarily increasing accuracy despite high precision (Dottori et al., 2013). Probabilistic flood maps have proven to be preferable to deterministic flood maps due to their representation of uncertainty (Teng et al., 2017). Probabilistic flood maps (e.g. Bates et al., 2004; Hall et al., 2011; Pappenberger et al., 2005; Romanowicz & Beven., 2003) show the likelihood of an area flooding as opposed to an area appearing as inundated or not in deterministic maps. Probabilistic flood maps do however require large numbers of model runs and for computationally intensive models this takes a prohibitively long time (Neelz & Pender., 2013).

Chapter 3 – Study Area

3.1 Location

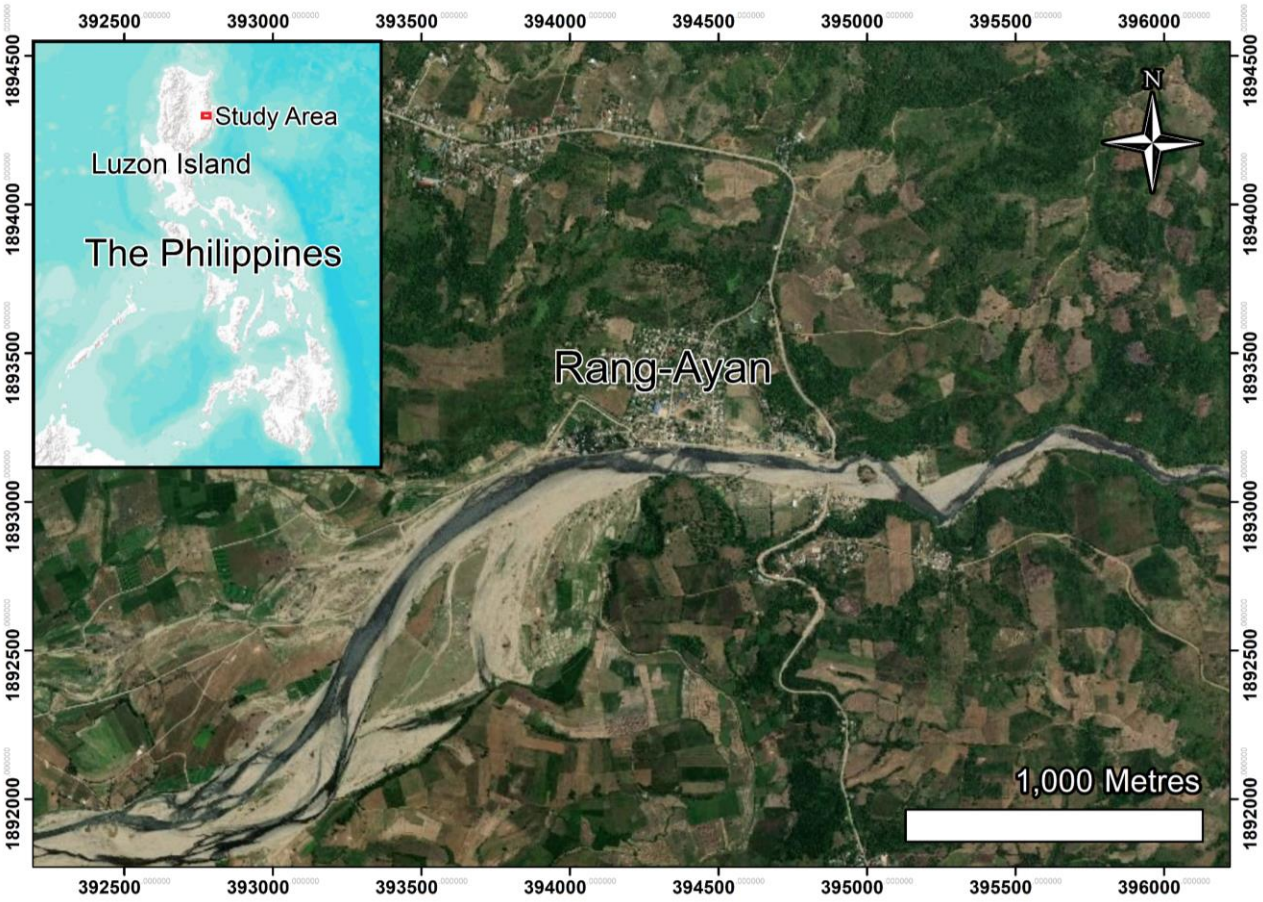

Figure. 3.1. *A map showing the study area, a section of the Bintacan de Ilagan River in Isabela Province, Luzon Island, the Philippines.*

The study area this dissertation will focus on is a section of the Bintacan de Ilagan (Bintacan) River located in Isabela Province, Luzon Island, the Philippines (Figure. 3.1.). The Bintacan is located on the East of Luzon island, the largest and most populated island within the Philippines (Census., 2015; UN., 2016). The Bintacan originates from the western slopes of the Sierra Madre mountain range, the longest mountain range within the country. The Bintacan is a tributary of the Pinacanauan de Ilagan (Ilagan) which is itself a tributary of the Cagayan, the longest river and the largest by discharge in the Philippines (Kimutai., 2018).

3.2 General Characteristics

The study area is approximately 9km^2 and is located at the edge of the Sierra Madre mountains. Within the study area the river's characteristics change from a confined mountainous section with higher gradient, to a lower gradient less confined section as it

flows onto alluvial plains. The catchment of the Bintacan consists of open forest in the upper reaches and cultivated land in the lower reaches (Paringit & Floresca., 2017) with the small town of Rang-Ayan located within the study area. The study area is representative of a small ungauged topographically complex tropical upland catchment.

3.3 River Morphology

The Bintacan is a tropical river, defined as a river which is located in the tropical climate belt, experiencing warm temperatures with little intra-annual variability and having high variation in seasonal precipitation (Dingle et al., 2019). However, the Ilagan River catchment experiences relatively subdued seasonality compared to other tropical rivers (Tolentino et al., 2016). Tropical rivers are usually characterised by high variation in seasonal discharge, large sediment loads and rapid changes in river morphology. The key controls on river morphology within the study area are the rate of sediment supply and the magnitude and frequency of flood events caused by typhoons (Dingle et al., 2019).

3.4 Geology

The mountains within the study area are characterised by Eocene to Oligocene bedded meta-volcanics, meta-sediments, and basaltic to andesitic flow deposits of the Caraballo Formation (Dingle et al., 2019). The soil in the study area is unconsolidated in the upper section and consists of sandy and clay loams within the lower section (Paringit & Floresca., 2017).

3.5 Super Typhoon Lawin

Super typhoon Lawin in October 2016 and the subsequent flooding caused considerable damage and morphological change within the study area. Figure. 3.5.A. shows satellite imagery from before the typhoon hit and Figure. 3.5.B. shows satellite imagery from after the typhoon. The main road bridge, two weirs/footbridges and ~10 houses were destroyed within the study area (Dingle et al., 2019).

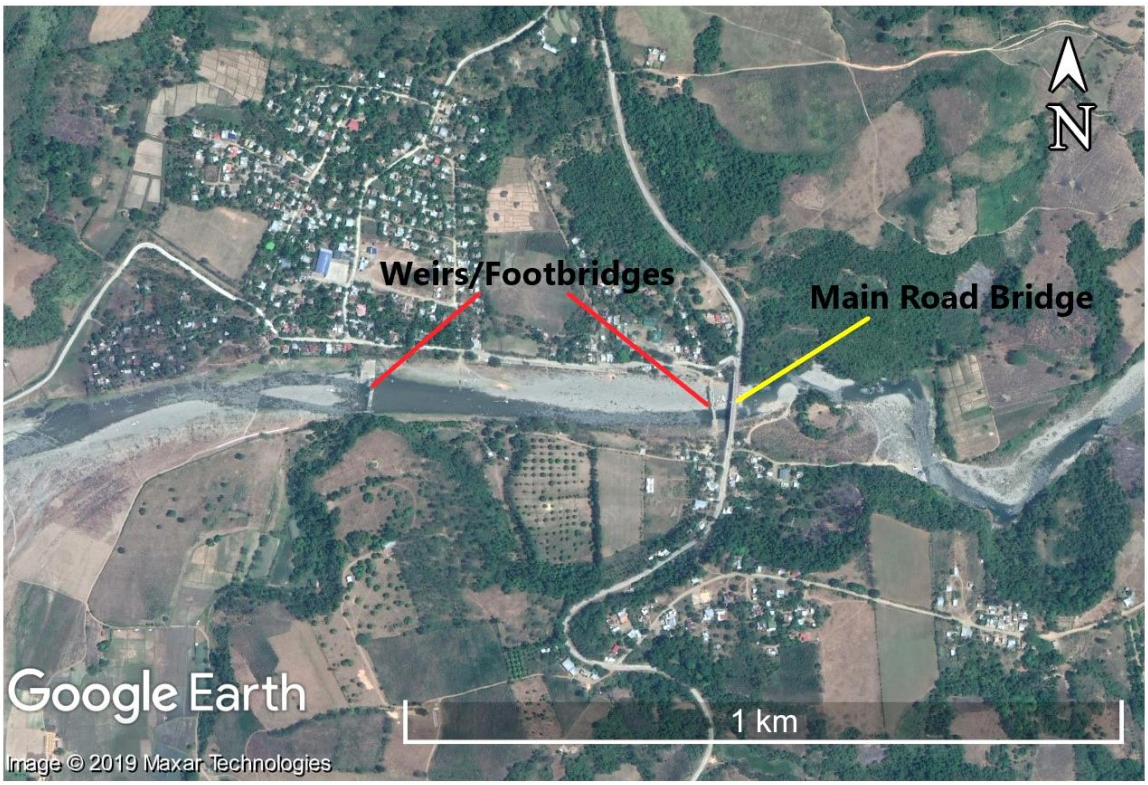

Figure. 3.5.A. *Satellite imagery from 18/04/2016 showing a section of the study area before super typhoon Lawin hit in October 2016.*

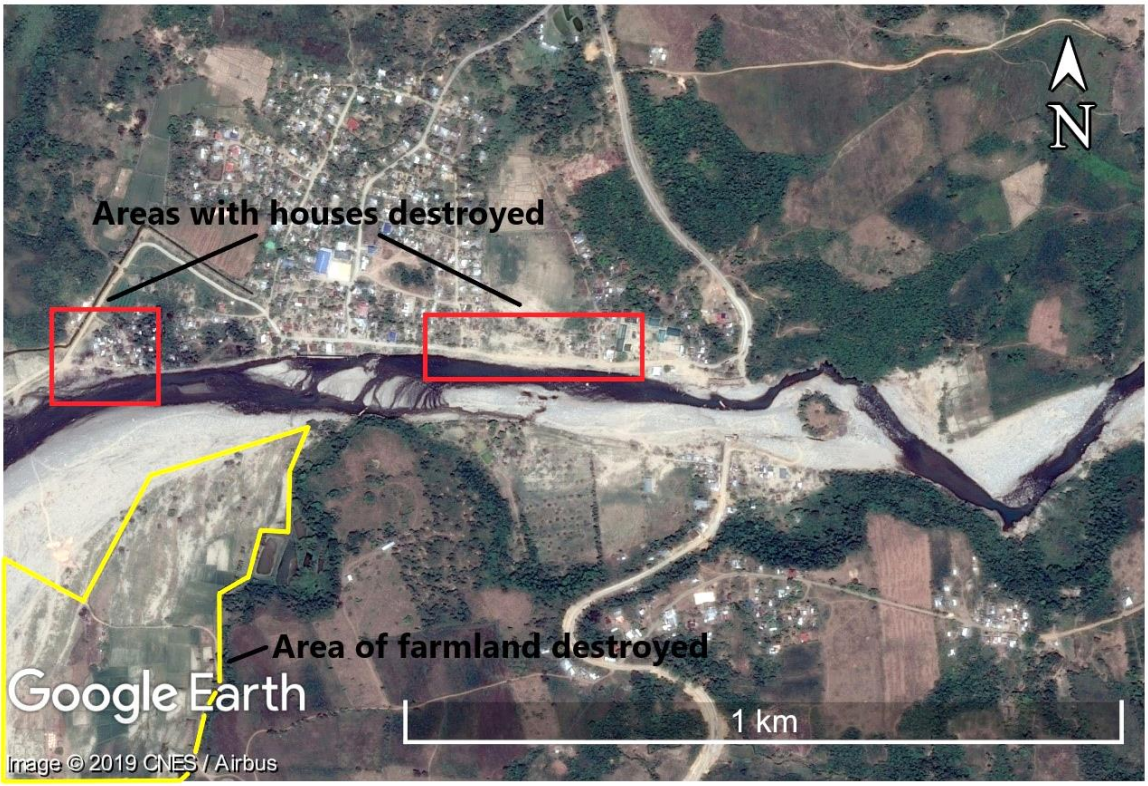

Figure. 3.5.B. *Satellite imagery from 13/04/2017 showing the same section of the study area after super typhoon Lawin hit. The two weirs/footbridges and the road bridge have been destroyed along within houses on the North bank of the river. An area of farmland has been destroyed including a larger area further downstream. Significant morphological change can also be observed.*

Chapter 4 – Methodology

4.1 Choice of Model

A hydraulic model was chosen over empirical methods due to empirical methods' inability to predict future flood events or alter model inputs and variables to perform scenario analysis (Teng et al., 2017). A hydrodynamic model was chosen over a simple conceptual model due to simple conceptual models' lack of representation of flow dynamics (Neelz & Pender., 2013). This was problematic due to the nature of the study area, as simple conceptual models struggle in topographically complex and hydraulically complex floodplains (Afshari., 2018., Neelz & Pender., 2013; Teng et al., 2017). A 1D/2D linked hydrodynamic model was chosen, modelling the river channel in 1D and the floodplain in 2D, to take advantage of both 1D models' ability to effectively model in-channel flow (Tayefi et al., 2007) and 2D models' ability to effectively model floodplain flow (Neelz & Pender., 2010; Neelz & Pender., 2013; Tayefi et al., 2007). A 1D/2D model was decided to be the best choice for the study area as 1D/2D models have been determined to be optimal for modelling in topographically complex floodplains, especially in upland areas (Tayefi et al., 2007). The software chosen to produce the model was Flood Modeller due to its capabilities in creating 1D/2D linked hydrodynamic models and because the software is freely available (Jacobs., 2019).

4.2 Flood Modeller

Flood modeller 1D/2D linked models function as described in sections 2.2.2.1, 2.2.2.2 and 2.2.2.4 of the literature review. The 1D model covering the river channel handles the discretisation of space as a series of cross-sections and the one-dimensional Saint-Venant equations (Figure. 2.2.2.1.) are solved to calculate water levels and flow at each cross-section (Jacobs., 2019). The 1D model makes assumptions about the one-dimensionality of flow, uniformity of velocity and horizontality of water level across cross-sections (Jacobs., 2019; Tayefi et al., 2007). However, these assumptions were deemed appropriate when modelling in-channel flow (Tayefi et al., 2007). The 2D model covering the floodplain handles the discretisation of space as a structured grid and the two-dimension Saint-Venant equations (Figure. 2.2.2.2.) are solved to calculate water levels and velocity of flow (Jacobs., 2019). The 2D model makes the assumption that water depth is shallow compared to the other two dimensions (Jacobs., 2019) and this

was deemed appropriate upon analysis of the study area's topography. The Flood Modeller standard ADI solver was chosen over the TVD solver as the TVD solver was deemed unnecessary for the study area. The study area was not exceptionally steep, and it was determined that hydrological shocks would not significantly affect results with Froude numbers likely staying below 1 (Jacobs., 2019). The ADI solver is also significantly faster computationally so more appropriate given the large number of model runs (Jacobs., 2019).

4.3 Data Acquisition

Topographic and bathymetric data was collected for the study area by the University of the Philippines as part of the Disaster Risk and Exposure Assessment for Mitigation (DREAM) Program (Paringit & Floresca., 2017). Data was obtained using light aircraft-based LiDAR and ground based bathymetric survey and a 1m resolution DEM was produced with 50cm and 20cm horizontal and vertical accuracies, respectively (Paringit & Floresca., 2017).

4.4 Building the Model

The DEM was cut to only include the study area and resampled to 5, 10, 15, 20 and 25m resolutions in QGIS. The 5m DEM was used for the majority of modelling and the other resolutions were only used for sensitivity analysis. Cross-sections were then created at 50m intervals along the river channel using the 5m DEM as the input (e.g. Figure. 4.4.) and these cross-sections were used to create the 1D model. Active area shapefiles were then produced to show the computer the areas to model in 2D for the floodplain. Lateral link lines were then produced to link the 1D in-channel model with the 2D floodplain model. A downstream boundary, parallel and in line with the last 1D cross-section, was also created for water to flow out of the model. The downstream boundary was a normal depth boundary and the slope was determined by analysing a slope map created in QGIS, with a normal depth slope of 0.002 chosen. The 5m DEM, active areas, link lines and downstream boundary were then used as inputs for the 1D/2D linked model.

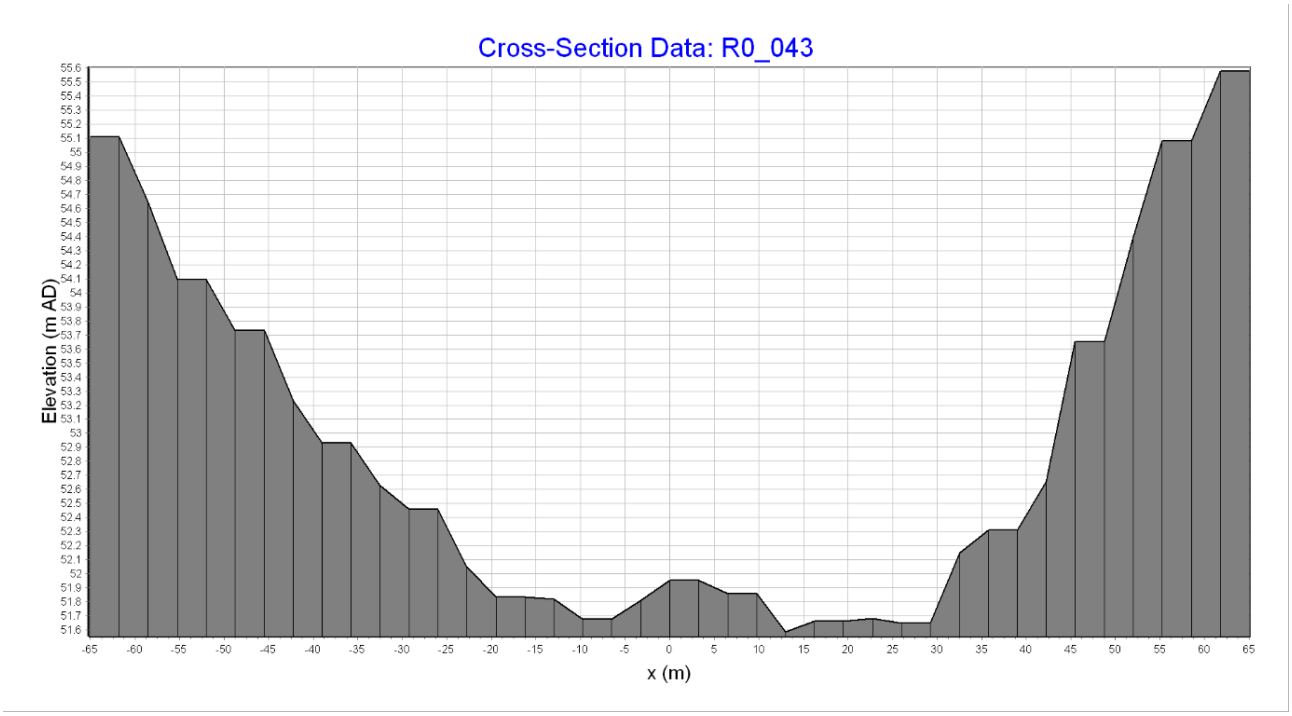

Figure. 4.4. *An example of a cross-section used within the 1D model showing the elevation of the river channel along that cross-section. Note that the x and y axis are not at the same scale and river depth is distorted for visualisation purposes.*

4.5 Model Testing

The 1D model was then tested for a range of steady and unsteady inflow values to assess model stability and convergence. The model displayed good stability and reasonable convergence, with convergence values within Flood Modeller's tolerance level. The 1D/2D linked model was then tested for a range of unsteady inflows to assess results and issues were encountered relating to the length and number of cross-sections. The model was remade several times to change cross-sections, link lines and active areas with more cross-sections added to improve convergence further. Model testing was undertaken after each remake. A satisfactory model was reached when no issues were encountered with the cross-sections and when the model had reached very good convergence – well within Flood Modeller's tolerance levels.

4.6 Low Flow Estimation

No river flow data was available for the study area, so estimations of model inflow had to be made. Low flow values for the river were estimated using satellite imagery, street view (Google Earth Pro), on the ground photography and the equation for river flow (Figure. 4.6.).

$$Q = w \times d \times v$$

Figure. 4.6. *A box containing the equation for river flow (Hedman & Osterkamp., 1982). Q represents the flow of water (m^3/s), d represents the average depth of water in a river cross-section (m), w represents the width of the cross-section (m) and v represents the velocity of water moving through the cross-section (m/s).*

Low flow values for d and v were estimated using the on the ground photography and street view (2016). h was estimated to be between 0.5 and 0.75m and v was estimated to be approximately 1m/s based upon the nature of the river in the study area (Thome & Zevenbergen., 1985). The width of the river in low flow was determined using satellite imagery from the year the LiDAR for the DEM was captured (2016). Measurements for w were taken at each of the three sections of river for which there was on the ground photography and street view available with w values ranging from 30-40m. Given the estimations of d, v and w it was determined that a reasonable value for Q for low flow was 20 m^3/s.

4.7 Low Flow Model Calibration

The 1D model was then run for a steady inflow value of 20 m^3/s. Low flow model calibration was undertaken by altering in-channel roughness values for the 1D model, producing a low flow inundation area for each roughness value tested (Figure. 4.7.A.). These low flow inundation areas were then visually compared to satellite imagery from 2016 using Google Earth Pro, and the in-channel roughness value which produced the closest low flow inundation area to the satellite imagery was a Manning's n value of 0.03 (Figure. 4.7.B.). The model run with a steady inflow of 20 m^3/s and in-channel roughness of 0.03 was then used as the low flow initial conditions for any unsteady flow model runs.

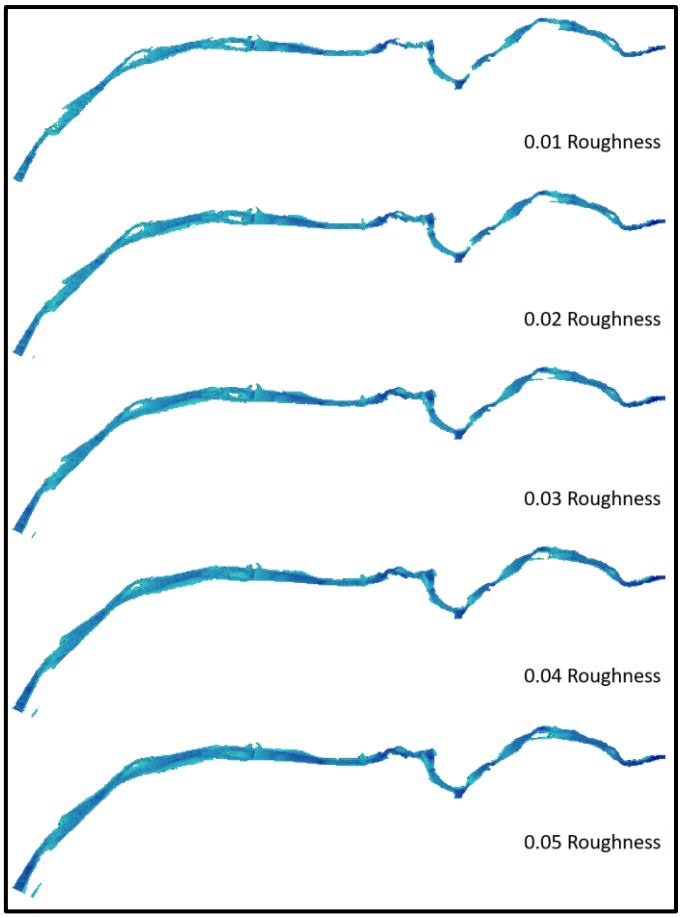

Figure. 4.7.A. *A figure showing the low flow inundation area for varied in-channel roughness values. In-channel roughness values were varied between 0.01 and 0.05 at 0.005 increments with 0.01 increments shown here for visual representation.*

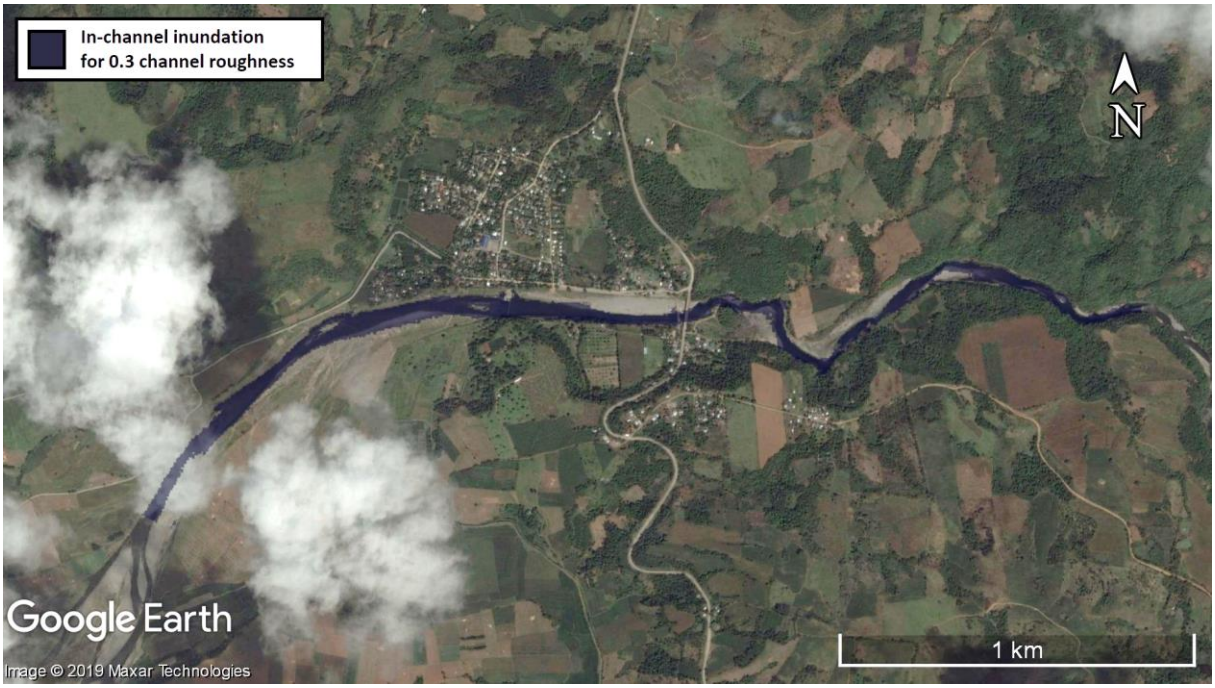

Figure. 4.7.B. *A map showing the low flow inundation area for an in-channel roughness value of 0.03 compared to low flow satellite imagery from when the year the LiDAR data was collected (2016).*

4.8 High Flow Model Calibration

High flow model calibration or validation was not able to be undertaken due to the lack of calibration data available. There was no flow data for the Bintacan for any high flow events and no satellite imagery data available to calibrate the model. Therefore, high flow model calibration by altering the floodplain roughness to best fit satellite imagery was not possible.

4.9 Roughness Estimation

Due to the lack of calibration data, the floodplain roughness was estimated using satellite imagery, street view and on the ground photography. Using Chow., 1959 and Arcement & Schneider., 1989 as guidance, floodplain roughness values were estimated based upon the land use and density of vegetation in the study area. Also taken into account was the fact that the DEM had been processed and scrubbed of houses and other manmade structures (Paringit & Floresca., 2017), artificially reducing the DEM roughness. It was determined a Manning's n roughness value of 0.12 was appropriate for the study area due to the dense vegetation in the upper section and to compensate for the artificial reduction of roughness in the town. This roughness value is likely too high for the lower section of the study area, which is primarily cultivated land, but was chosen to best represent flood inundation in the town and upper section of the study area, as the focus of this dissertation is to assess flood risk, making prioritising model accuracy for the town an obvious choice.

4.10 – Sensitivity Analysis – Model Variables and Inputs

Local sensitivity analysis was undertaken on the model to assess how altering model variables and inputs affected total flood inundation area. Local sensitivity analysis was chosen due to the computationally intensive and complex nature of the model. It was determined that due to high model run times and the high number of model variables, global sensitivity analysis would take a prohibitively long time (Neelz & Pender., 2013; Teng et al., 2017). The aim of the sensitivity analysis was to determine which variables and inputs had the largest effect on model results for a representative high flow event, and to help understand the uncertainties associated with model results (Beven et al., 2015; Dottori et al., 2013; Teng et al., 2017).

The variables and inputs altered for sensitivity analysis were the floodplain roughness, the model timestep, the resolution of the DEM and the slope of the normal depth boundary. Although not studied extensively in the literature it was decided that undertaking sensitivity analysis on the model timestep and normal depth slope was worthwhile as both were subjective decisions which could introduce uncertainty. Each variable was altered one at a time around a baseline set of variables which had a floodplain roughness of 0.12, a model timestep of 2s, a DEM resolution of 5m and a normal depth boundary slope of 0.002. The input hydrology was kept constant using a simple representative high flow event (Figure. 4.10.). The magnitude and duration of this event were chosen based upon volume of estimated flow for the Ilagan (relative to the size of the Bintacan) for a synthetic high flow event (Paringit & Floresca., 2017) – with the representative event producing significant, but not complete, inundation of the floodplain allowing variables affects to be assessed effectively.

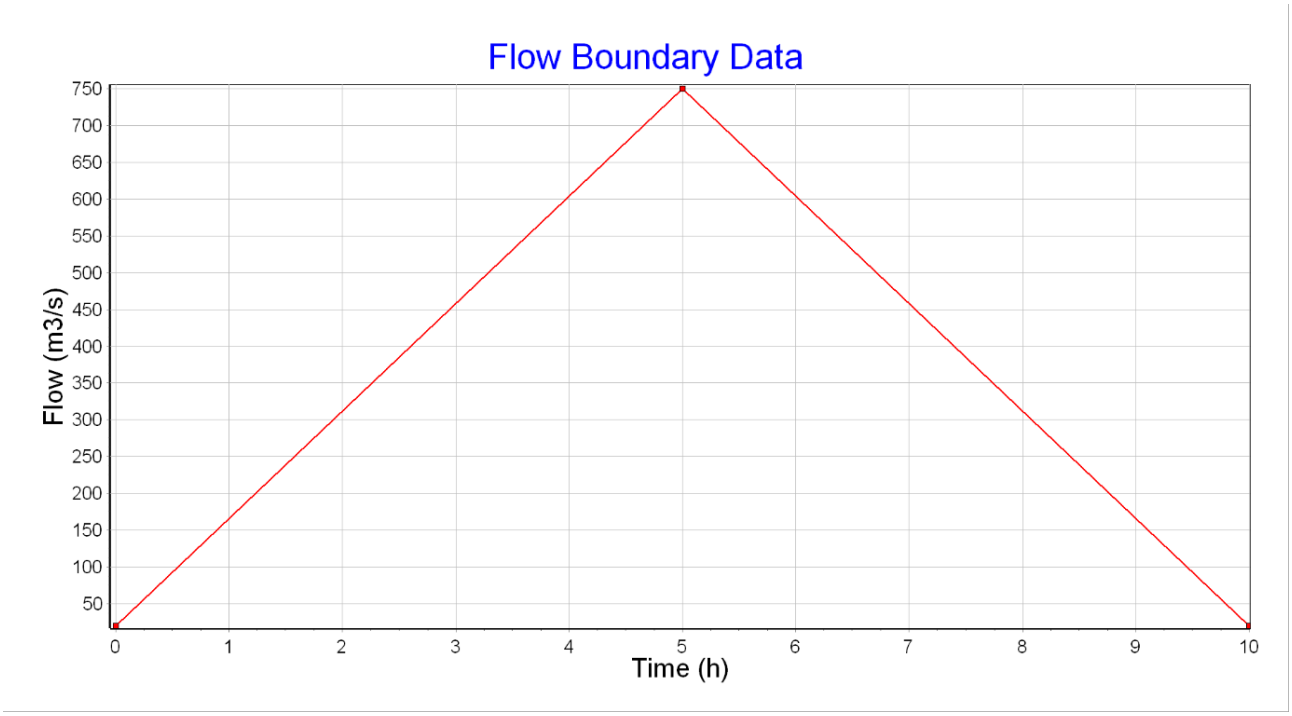

Figure. 4.10. *The baseline input hydrograph used for undertaking sensitivity analysis. The hydrograph has a peak flow of 750 m^3/s, a time to peak of 5 hours, a total high flow event duration of 10 hours and a total event volume of 3750 m^3 plus 200m^3 of volume from the low flow initial conditions.*

The floodplain roughness was varied between values of 0.01 to 0.2 at 0.01 increments for the Manning's n to assess the effect changing floodplain roughness had on model results. The model timestep was varied between 0.25 and 5 seconds at 0.25s increments to assess what effect the model timestep had on results. The DEM resolution was varied

between 5 and 25m to assess the effect reducing DEM resolution had on model results. This was done by recreating the 1D/2D model four times, following the steps described in section 4.4 and using the lower resolution resampled DEMs as inputs. The same shapefiles used in section 4.4 were used again to ensure that the only effect being analysed was the change in DEM resolution. The normal depth boundary slope was varied between 0.001 and 0.003 to assess the effect changing the slope had on model results.

4.11 – Sensitivity Analysis – Input Hydrology

Hydrological sensitivity analysis was undertaken to assess what effects altering input hydrology would have upon total flood inundation and to help understand the uncertainties associated with model results (Beven et al., 2015; Dottori et al., 2013; Teng et al., 2017). To assess this the representative input hydrograph (Figure. 4.10.) was varied in two ways (while keeping constant the baseline set of model variables used in section 4.10). Firstly, the total event duration was varied from 4 to 24 hours in 1 hour increments, keeping total inflow (area under the hydrograph) constant, to assess the affect this had on model results. This meant reducing total event duration increased peak flow of the hydrographs and increasing total event duration decreased peak flow (e.g. Figure. 4.11.A..). Secondly, from the review of the literature (section 2.3.3.4) it was determined that no studies found had assessed the effect of changing the time to peak of input hydrographs, while keeping total inflow constant. It was decided this would be worthwhile investigating to contribute to the literature in an area seemingly understudied. The time to peak flow for the input hydrograph was varied from 0.5 to 5 hours at 0.5 hour increments, keeping total inflow (area under the hydrograph) and total event duration constant (e.g. Figure. 4.11.B.), to assess the effect this had on model results.

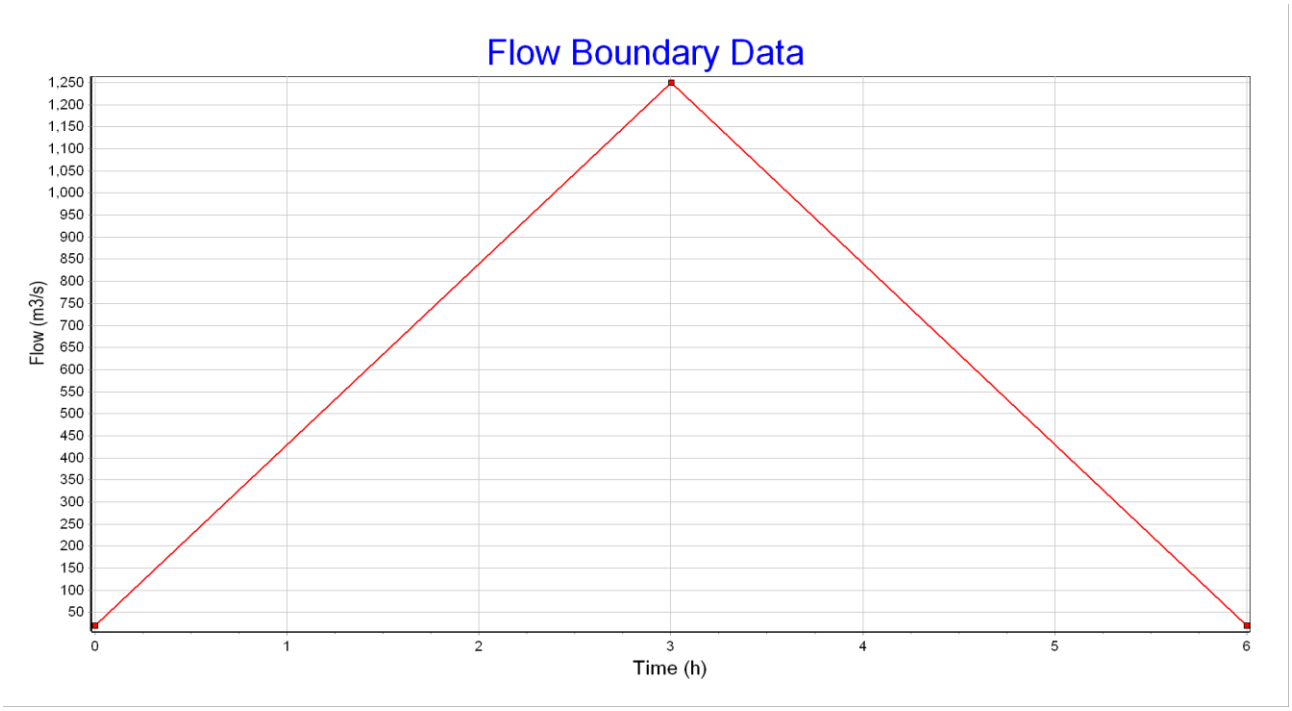

Figure. 4.11.A. *An example of an input hydrograph used for assessing the effect of total event duration for hydrological analysis. The hydrograph has a peak flow of 1250 m³/s, a time to peak of 3 hours, a total high flow event duration of 6 hours and a total event volume of 3750 m³ plus 160 m³ of volume from the low flow initial conditions.*

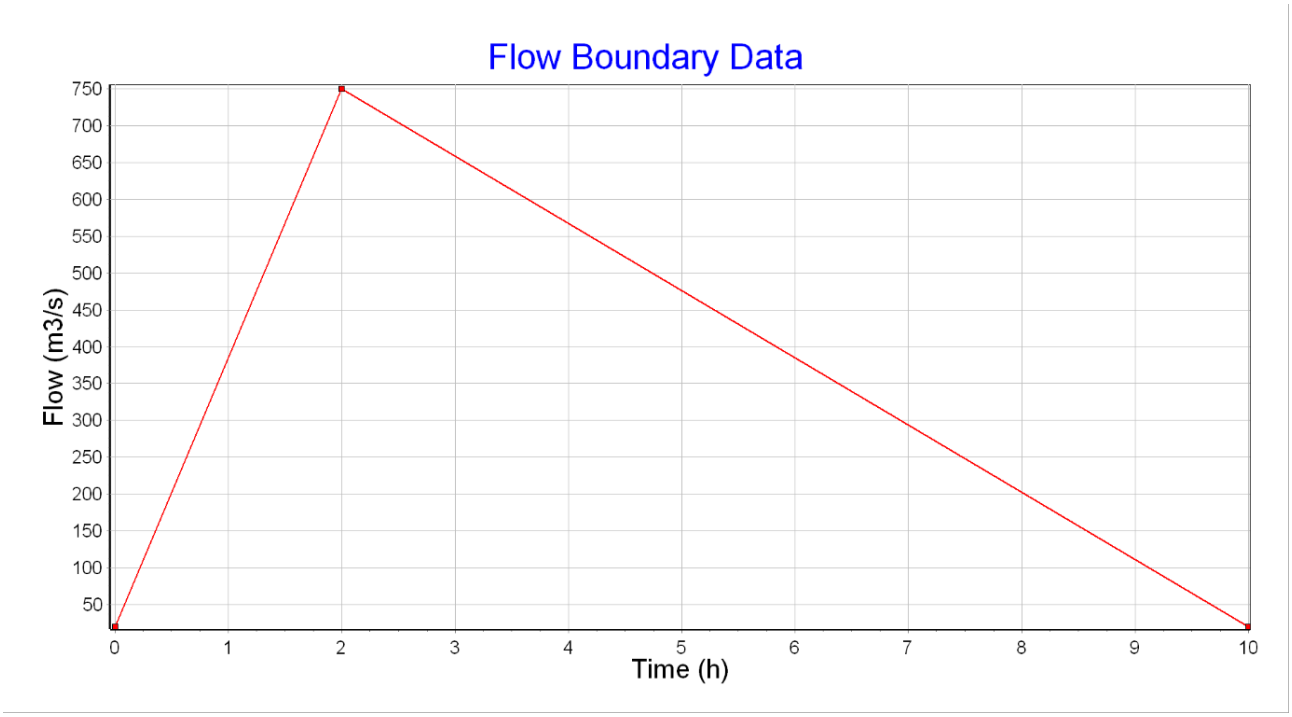

Figure. 4.11.B. *An example of an input hydrograph used for assessing the effect of time to peak for hydrological analysis. The hydrograph has a peak flow of 750 m³/s, a time to peak of 2 hours, a total high flow event duration of 10 hours and a total event volume of 3750 m³ plus 200 m³ of volume from the low flow initial conditions.*

4.12 – Estimating Return Period Flood Events

Due to the lack of flow data for the study area, hydrology for 5, 10, 25, 50 and 100-year return period flood events needed to be estimated. Peak flow values and event durations were estimated using data on return period flood events calculated for the Ilagan (Paringit & Floresca., 2017). The volume of water for the return period events for the Ilagan was calculated and scaled down for the Bintacan using the relative size of the two river catchments. This was deemed appropriate as the Bintacan catchment is located within the Ilagan catchment and therefore will experience similar rainfall patterns. The hydrograph shape (i.e. event duration and peak flow) for the Bintacan was estimated based upon the size and characteristics of the river catchment, with a shorter duration higher peak hydrograph estimated due to the steep mountainous nature of the catchment and smaller catchment size (Alexander., 1972; Heerdegen., 1974). These hydrographs were shorter and more intense than the one used in sensitivity analysis and therefore ideally, with more time, sensitivity analysis would have been carried out on each return period event. The shorter duration higher peak hydrographs (e.g. Figure. 4.12.) were deemed appropriate as the vast majority of rainfall in the return period events calculated for the Ilagan fell within 3-4 hours so the hydrograph peak flow would not be limited by rainfall intensity (Paringit & Floresca., 2017).

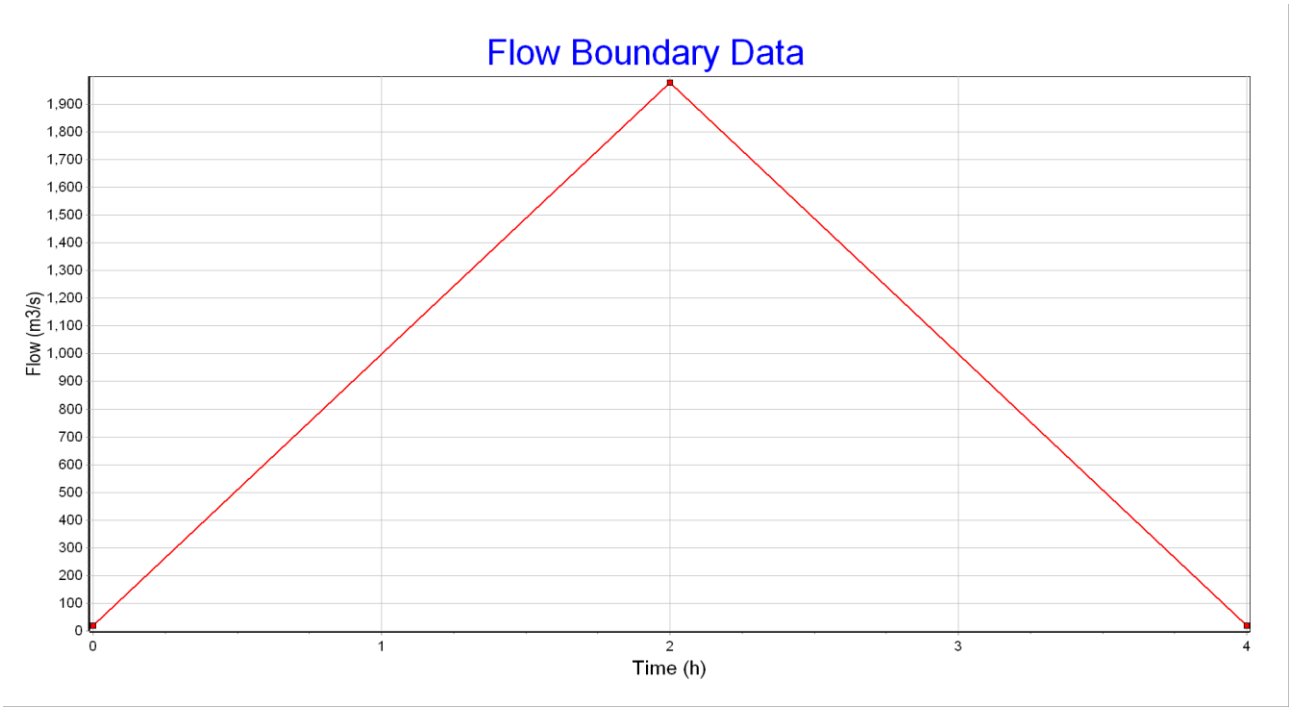

Figure. 4.12. *The input hydrograph used for the 100-year flood event production run. The hydrograph has a peak flow of 1977 m³/s, a time to peak of 2 hours, a total high flow event duration of 4 hours and a total event volume of 3954 m³ plus 80 m³ of volume from the initial conditions.*

4.13 – Final Production Runs

Final production runs were done for 5, 10, 25, 50 and 100-year flood events for the Bintacan using the estimated hydrology for these events as inputs. The model variables and inputs were 0.12 floodplain roughness, 2s model timestep, 5m DEM resolution and 0.002 downstream boundary normal depth slope. The output inundation areas for these events were then overlaid on Open Street Map data to calculate the number of buildings within the inundation area for each return period event. Total flood inundation maps were then produced, overlaying total inundation area on top of satellite imagery, for each return period flood event using ArcGIS. These return period inundation maps and Open Street Map were then used to assess flood risk in the study area.

Chapter 5 – Results

5.1 Sensitivity Analysis

5.1.1 Floodplain Roughness

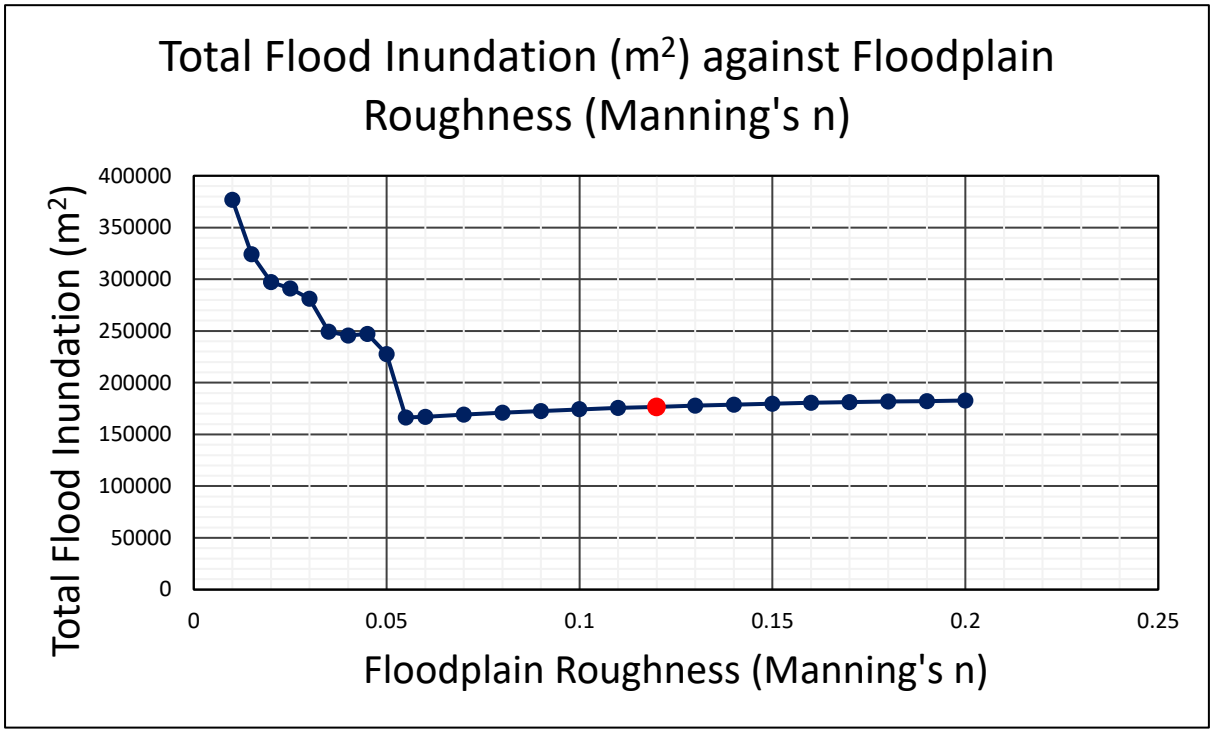

Figure. 5.1.1.A. *A graph showing the results of the sensitivity analysis undertaken varying the floodplain roughness. The graph shows how total flood inundation (m²) varies as the floodplain roughness value (Manning's n) is varied. The red point represents the baseline model run. Full table of results can be found in appendix A.*

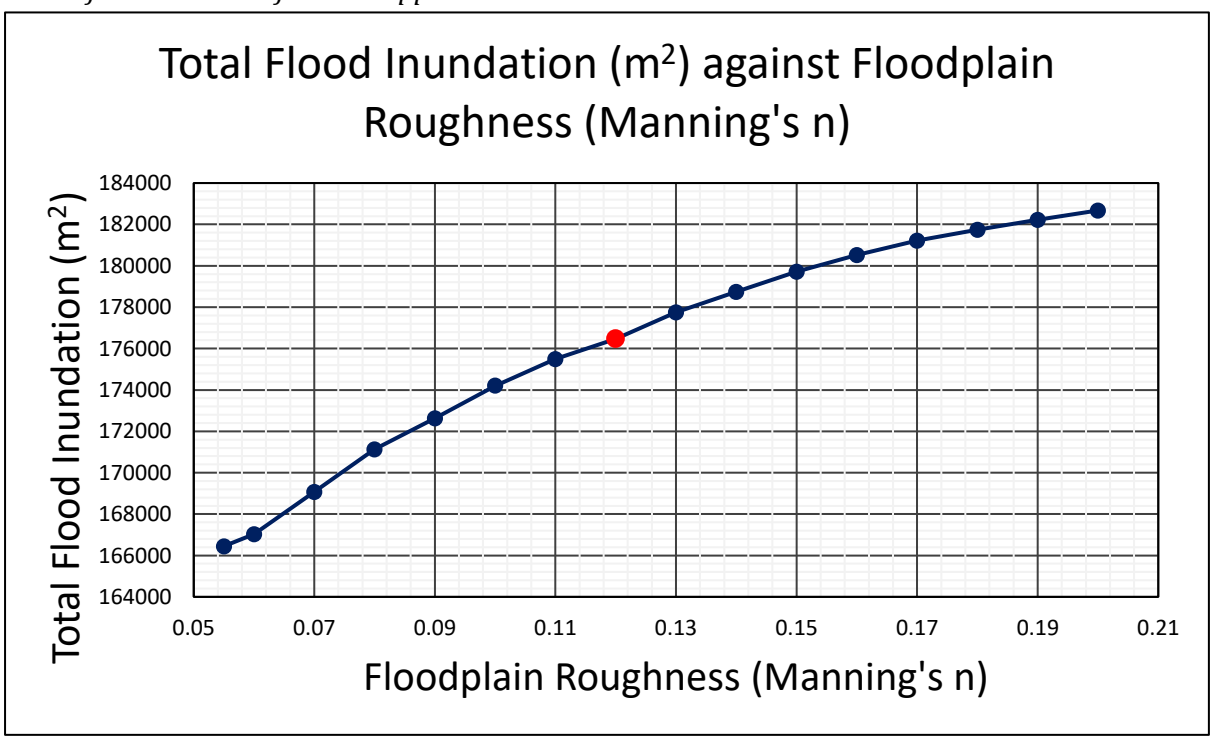

Figure. 5.1.1.B. *A graph showing the results of the sensitivity analysis undertaken varying the floodplain roughness in the range in which the model was stable. Note the y axis does not start from 0. The red point represents the baseline model run.*

The results from the sensitivity analysis undertaken altering floodplain roughness (Figure. 5.1.1.A.) show a linear trend of increasing total flood inundation with increasing floodplain roughness from values of 0.055 to 0.2. However, for floodplain roughness values of <0.055 the total flood inundation appears to sharply increase as floodplain roughness decreases and does not follow a clear trend. This was determined to be due to model instability which will be discussed later. Figure. 5.1.1.B. shows the relationship between floodplain roughness and total flood inundation in the stable range more clearly. In percentage terms the floodplain roughness does have a significant effect on total flood inundation. When floodplain roughness is reduced from 0.12 to 0.07 there is a 4.19% reduction in inundation area. When floodplain roughness is increased from 0.12 to 0.17 there is a 2.69% increase in inundation area.

5.1.2 Model Timestep

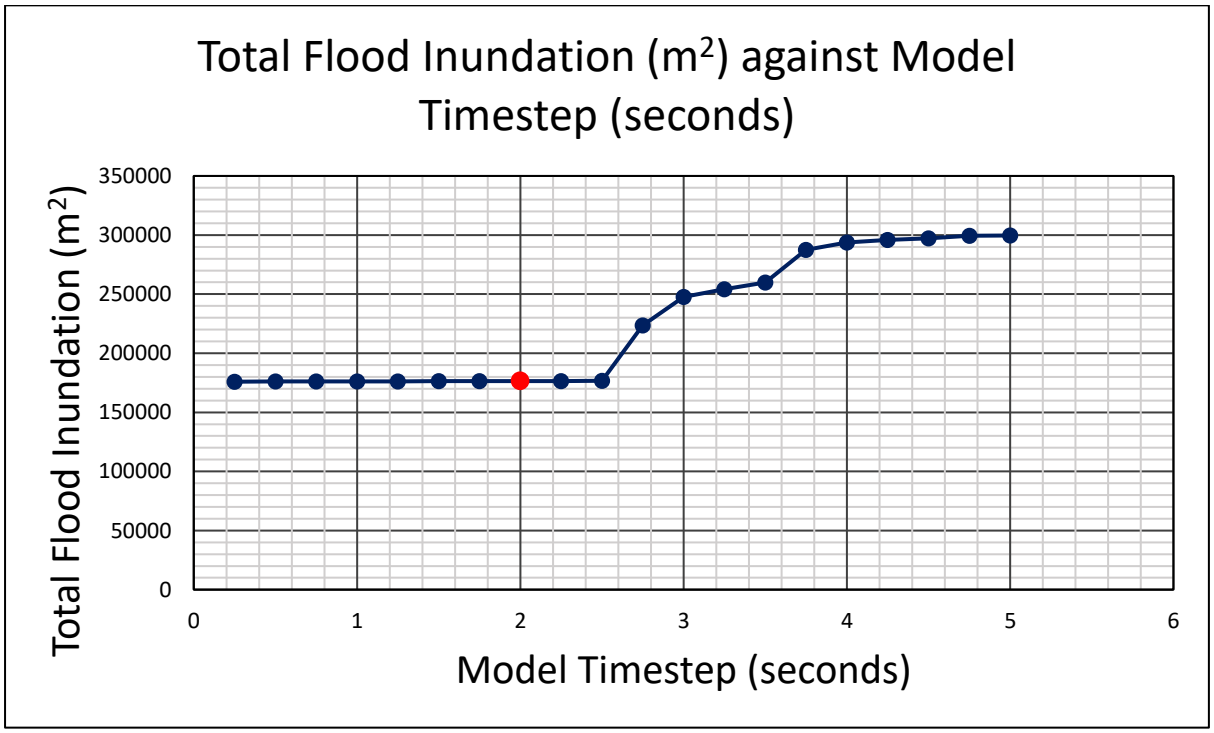

Figure. 5.1.2. *A graph showing the results of the sensitivity analysis undertaken varying the model timestep. The graph shows how total flood inundation (m²) varies as the model timestep (seconds) is varied. The red point represents the baseline model run. Full table of results can be found in appendix B.*

The results from the sensitivity analysis undertaken altering the model timestep (Figure. 5.1.2.) show little variation in total flood inundation between timesteps of 0.25s and 2.5s. However, for timesteps of >2.5s there is a sharp increase in total flood inundation as model timestep increases with no clear linear trend. This was determined

to be due to model instability which will be discussed later. In percentage terms altering the model timestep within the stable range has little effect on total flood inundation. When the model timestep is reduced from 2s to 0.25s there is a 0.33% decrease in total flood inundation. When the model timestep is increased from 2s to 2.5s there is a 0.071% increase in total flood inundation.

5.1.3 DEM Resolution

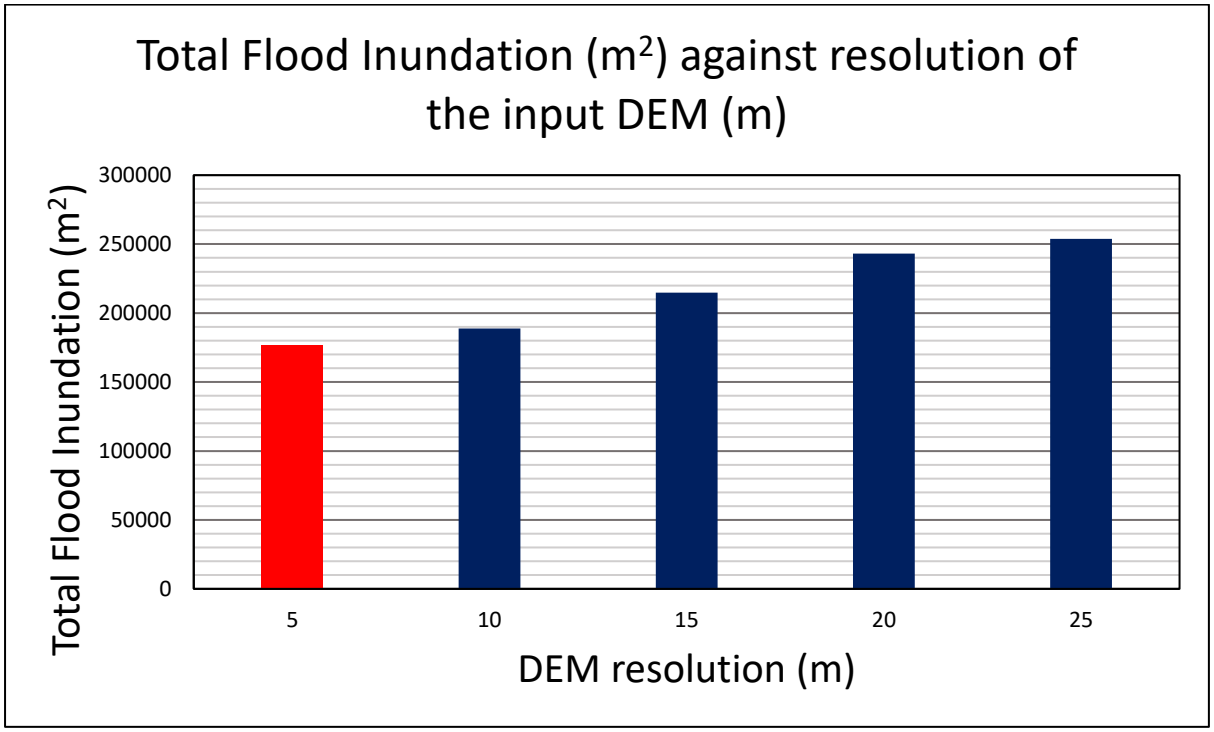

Figure. 5.1.3. *A graph showing the results of the sensitivity analysis undertaken varying the resolution of the input DEM. The graph shows how total flood inundation (m²) varies as the DEM grid size (m) is increased. The red bar represents the baseline model run. Full table of results can be found in appendix C.*

The results from the sensitivity analysis undertaken altering the resolution of the input DEM show a trend of increasing total predicted inundation area with increasing DEM grid size (Figure. 5.1.3.). An increase from a 5m to a 10m DEM caused a 7.04% increase in predicted flood inundation area. An increase from a 5m to a 15m DEM caused a 21.76% increase in inundation area. An increase from a 5m to a 20m DEM caused a 37.8% increase in inundation area. An increase from a 5m to a 25m DEM caused a 43.8% increase in inundation area.

5.1.4 Normal Depth Slope

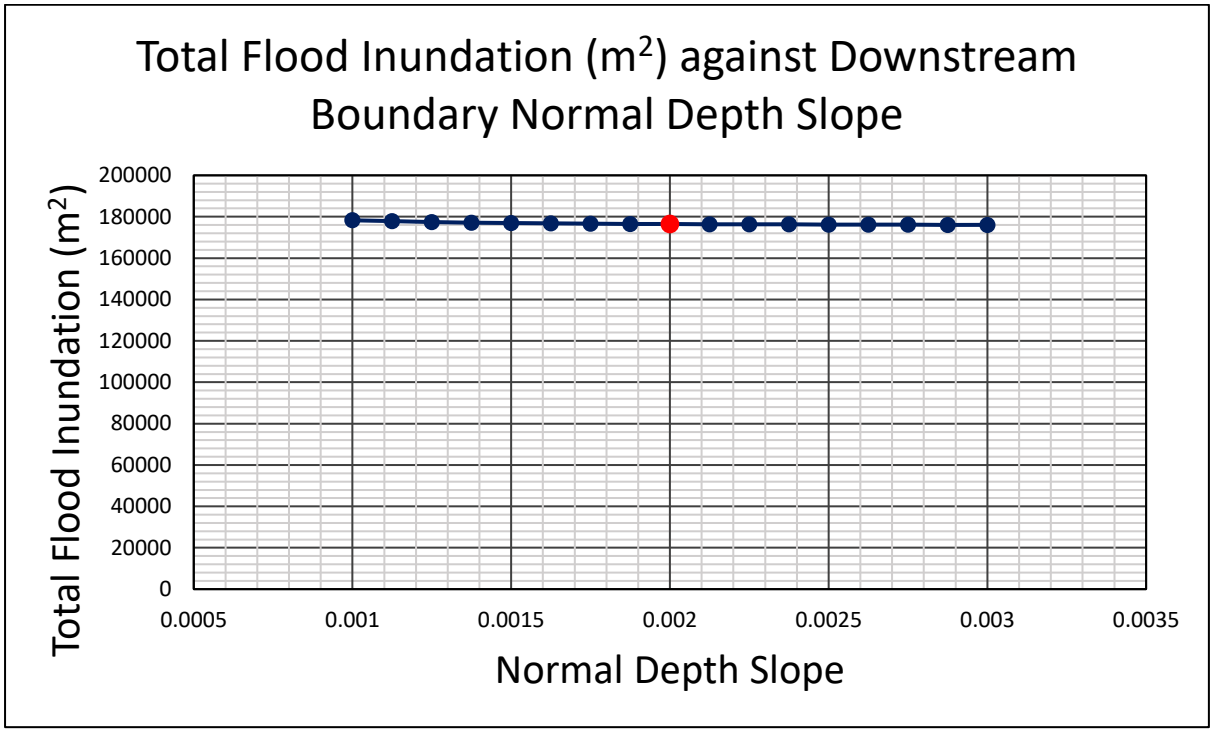

Figure. 5.1.4. *A graph showing the results of the sensitivity analysis undertaken varying the normal depth slope of the downstream boundary. The graph shows how total flood inundation (m^2) varies as the normal depth slope for the downstream boundary varies. The red point represents the baseline model run. Full table of results can be found in appendix D.*

The results from the sensitivity analysis undertaken altering the normal depth slope of the downstream boundary (Figure. 5.1.4.) show a linear trend of decreasing total flood inundation with increasing normal depth slope. In percentage terms altering the normal depth slope had little effect on total inundation area. When the slope is reduced from 0.002 to 0.001 there is a 1.02% increase in inundation area and when the slope is decreased from 0.002 to 0.003 there is only a 0.23% decrease in inundation area.

5.2 Hydrological Sensitivity Analysis

5.2.1 Time to Peak Flow

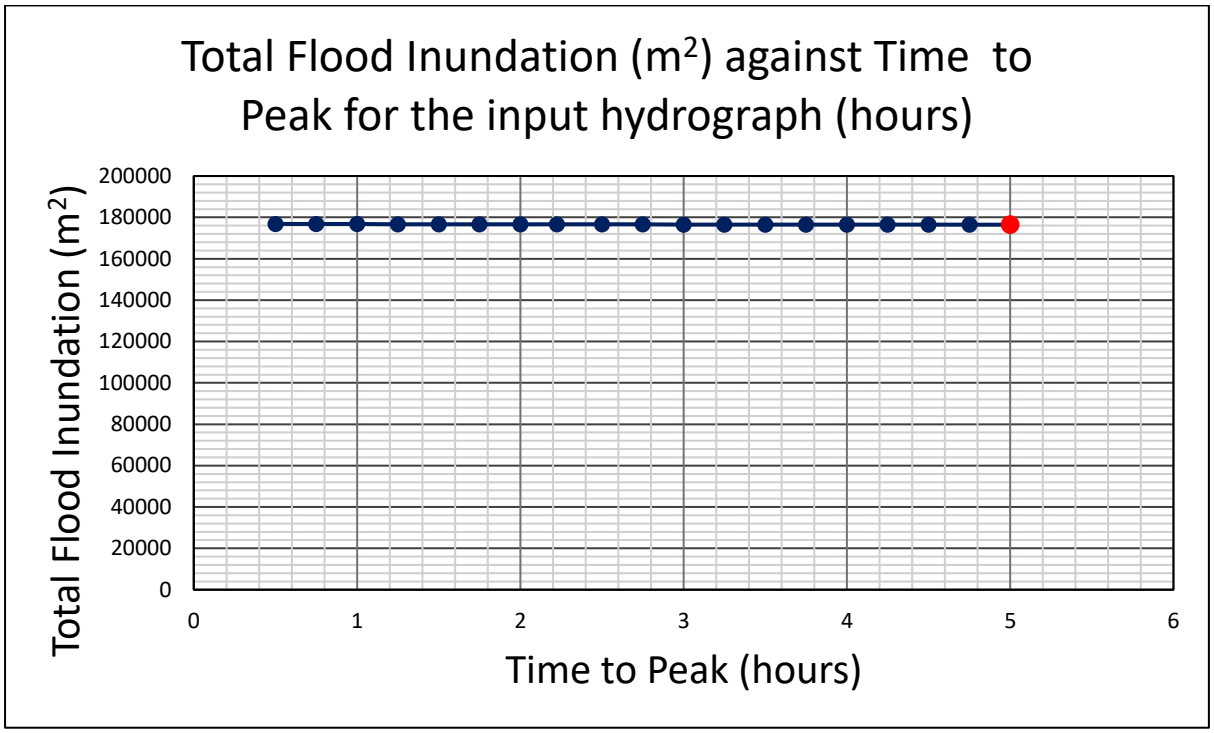

Figure. 5.2.1. *A graph showing the results of the hydrological analysis undertaken varying the time to peak (hours) for the input hydrograph, keeping total inflow volume constant. The graph shows how total flood inundation (m²) varies as the time to peak for the input hydrograph is varied. The red point represents the baseline model run. Full table of results can be found in appendix E.*

The results from the hydrological analysis undertaken altering the time to peak flow of the input hydrograph (keeping total volume of flow constant) (Figure. 5.2.1.) show very little variation in total flood inundation. This is consistent across all model runs from a time to peak of just 30 minutes to a time to peak of 5 hours in a 10 hour duration high flow event. In percentage terms the time to peak flow of the input hydrograph has little effect on total flood inundation area. When the time to peak flow is reduced from 5 hours to 30 minutes there is only a 0.21% decrease in inundation area.

5.2.2 Total Event Duration

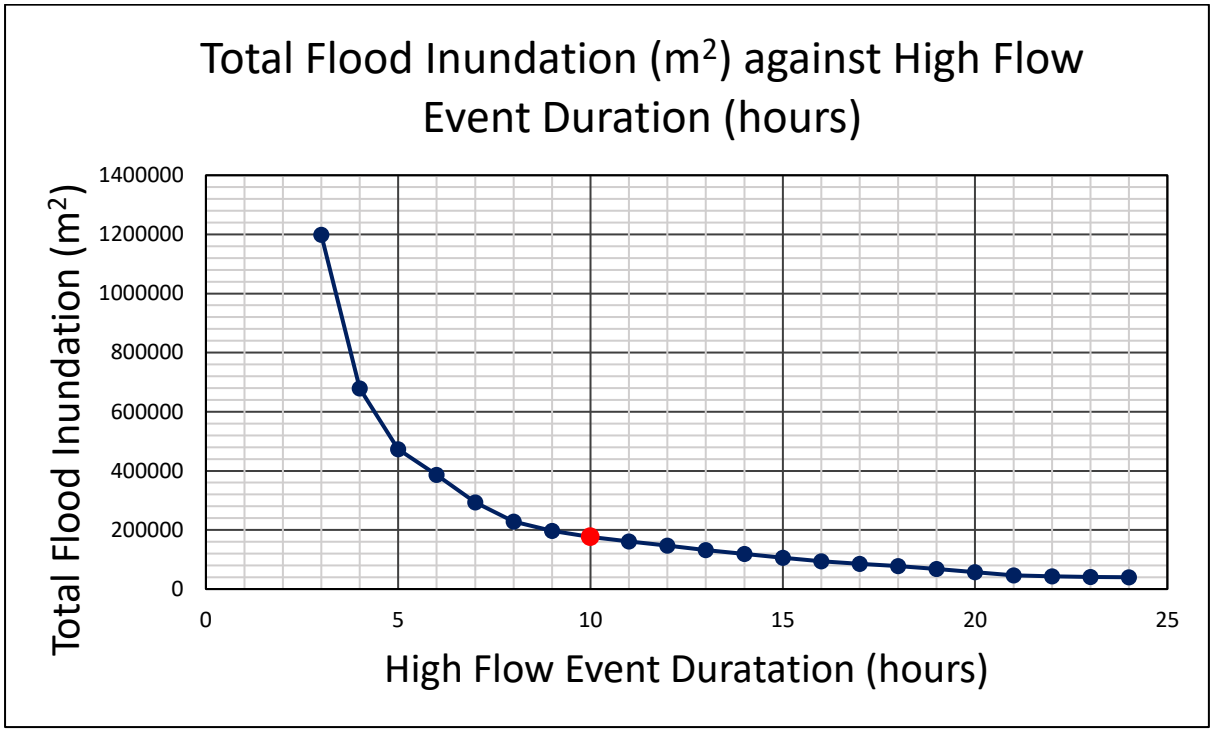

Figure. 5.2.2. *A graph showing the results of the hydrological analysis undertaken varying the total event duration (hours) for the input hydrograph, keeping total inflow volume constant. The graph shows how total flood inundation (m²) varies as the total event duration (hours) for the input hydrograph is varied. The red point represents the baseline model run. Full table of results can be found in appendix F.*

The results from the hydrological analysis undertaken altering the total event duration while keeping total volume of flow constant i.e. altering the intensity and duration of the flood event (Figure. 5.2.2.) show a trend of decreasing total flood inundation as total event duration increases. The total flood inundation is decreasing at a decreasing rate as total event duration increases. In percentage terms the total event duration has a larger effect on inundation area for shorter duration high flow events. A decrease in total event duration from 5 to 3 hours causes a 153.4% increase in inundation and a decrease in total event duration from 5 to 4 hours causes a 43.5% increase in inundation. Whereas for longer duration high flow events an increase in total event duration from 10 to 12 hours causes a 16.67% decrease in inundation and a decrease in total event duration from 20 to 24 hours causes a 7.52% decrease in inundation.

5.3 Production Runs

5.3.1 5-Year Flood

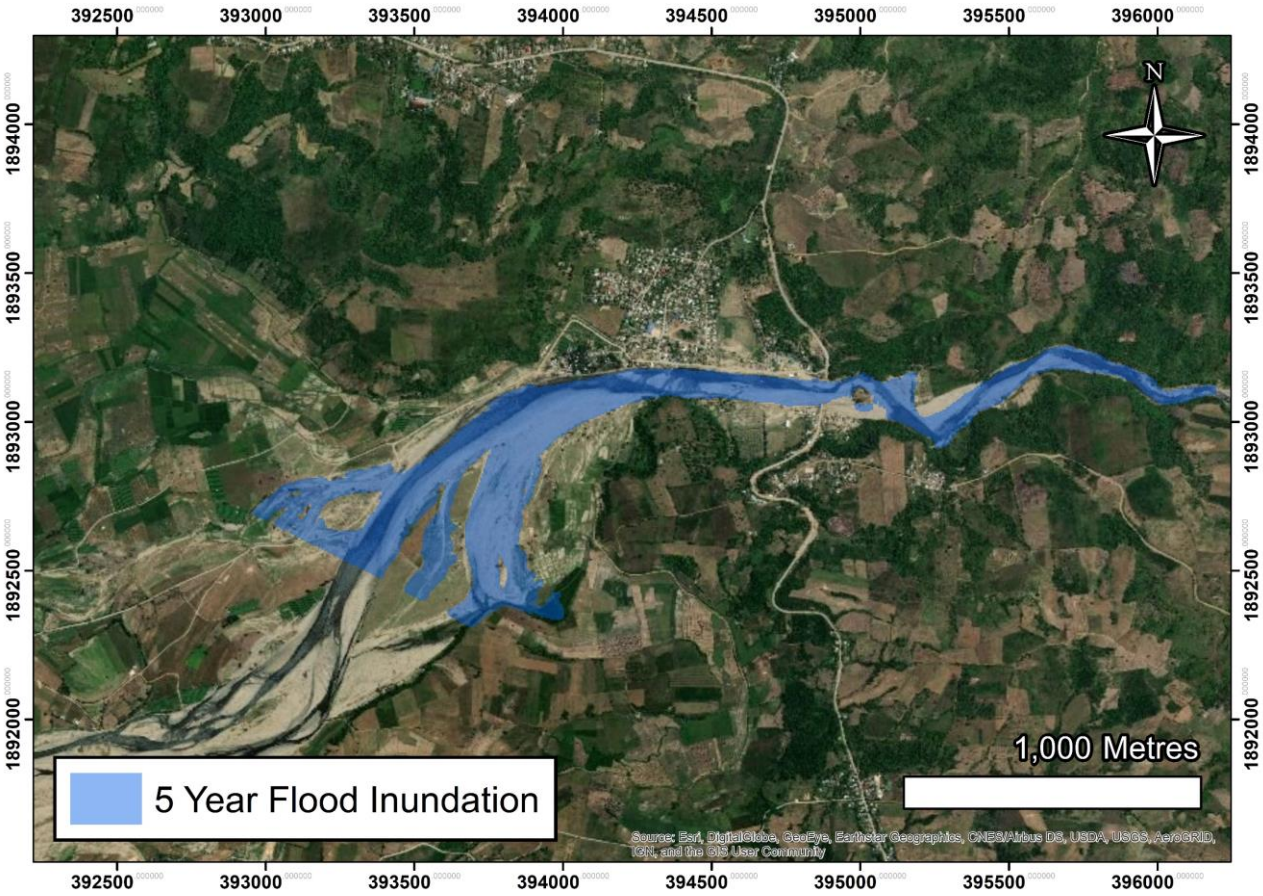

Figure. 5.3.1. *A map showing the total flood inundation in the study area for a flood with a 5-year return period.*

The results for a 5-year return period flood event show a total flood inundation area of 191500m^2 with 4 buildings at risk of flooding (Figure. 5.3.1.).

5.3.2 10-Year Flood

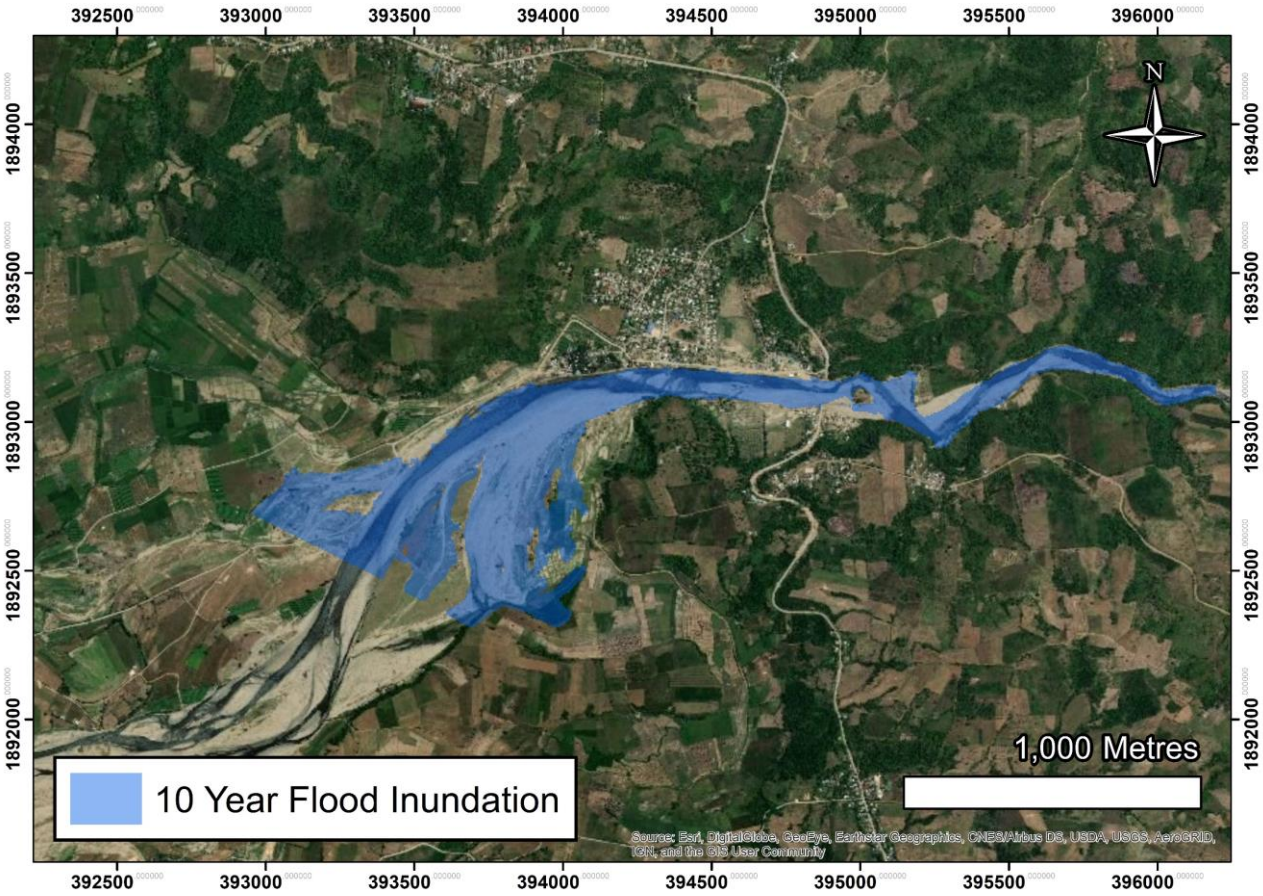

Figure. 5.3.2. *A map showing the total flood inundation in the study area for a flood with a 10-year return period.*

The results for a 10-year return period flood event show a total flood inundation area of 297725m^2 with 6 buildings at risk of flooding (Figure. 5.3.2.).

5.3.3 25-Year Flood

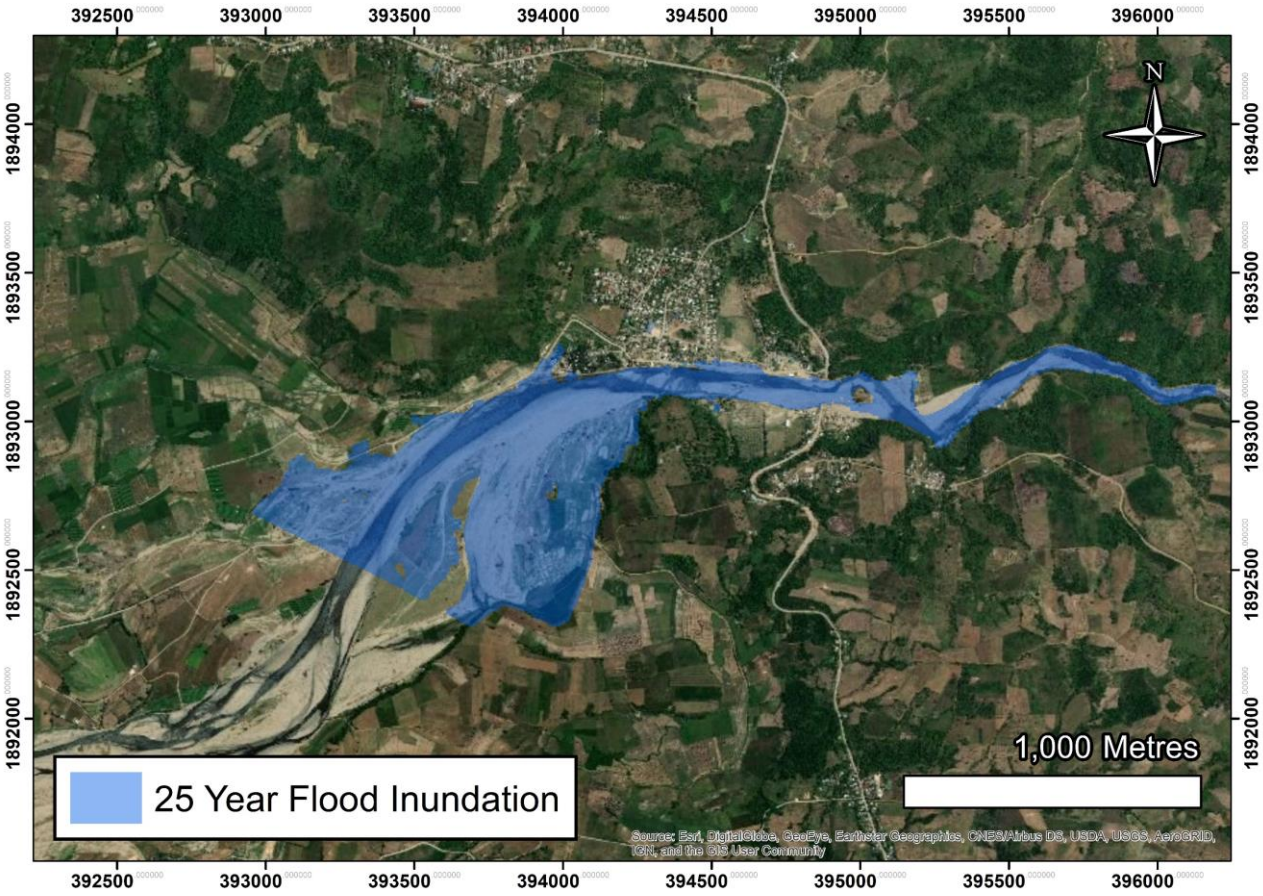

Figure. 5.3.3. *A map showing the total flood inundation in the study area for a flood with a 25-year return period.*

The results for a 25-year return period flood event show a total flood inundation area of 451525m^2 with 23 buildings at risk of flooding (Figure. 5.3.3.).

5.3.4 50-Year Flood

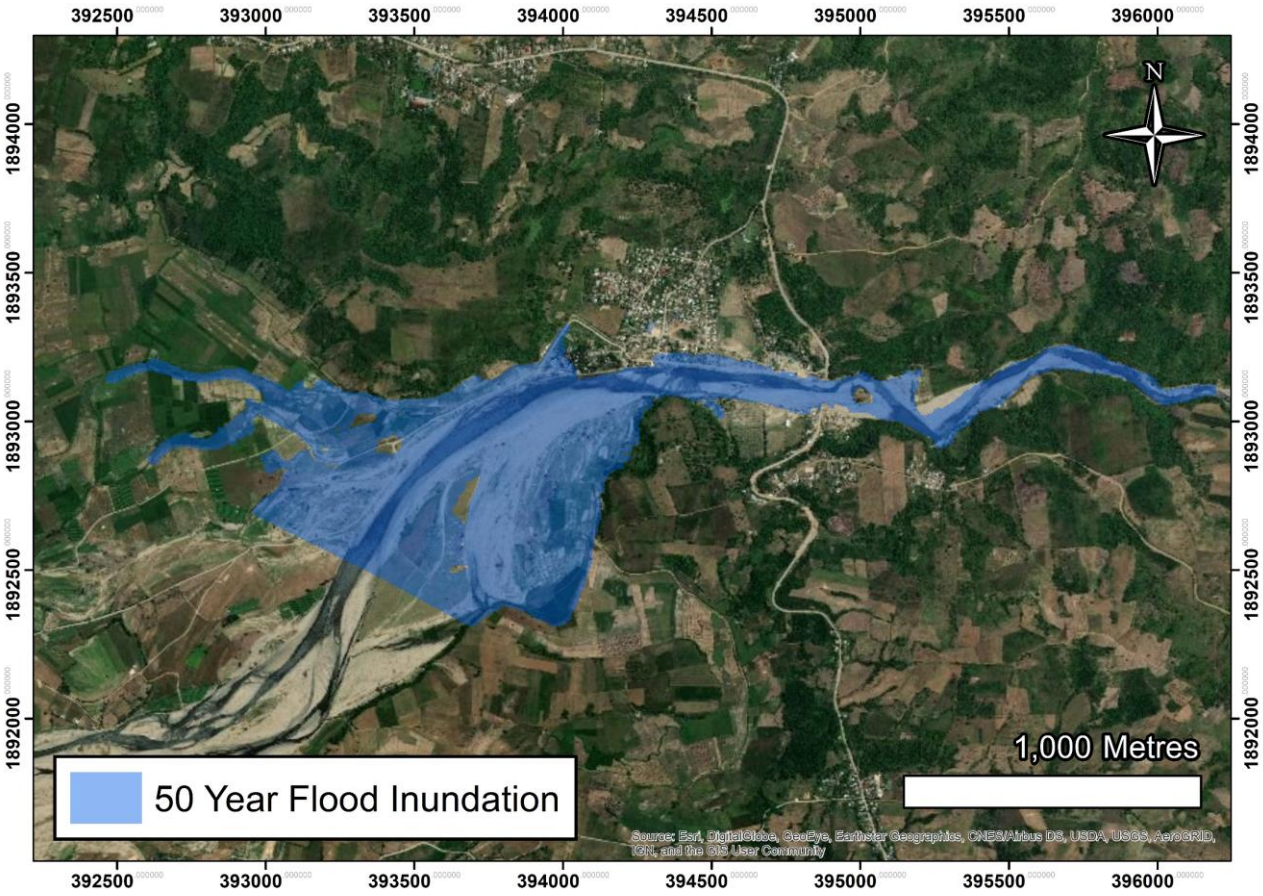

Figure. 5.3.4. *A map showing the total flood inundation in the study area for a flood with a 50-year return period.*

The results for a 50-year return period flood event show a total flood inundation area of 632925m^2 with 56 buildings at risk of flooding (Figure. 5.3.4.).

5.3.5 100-Year Flood

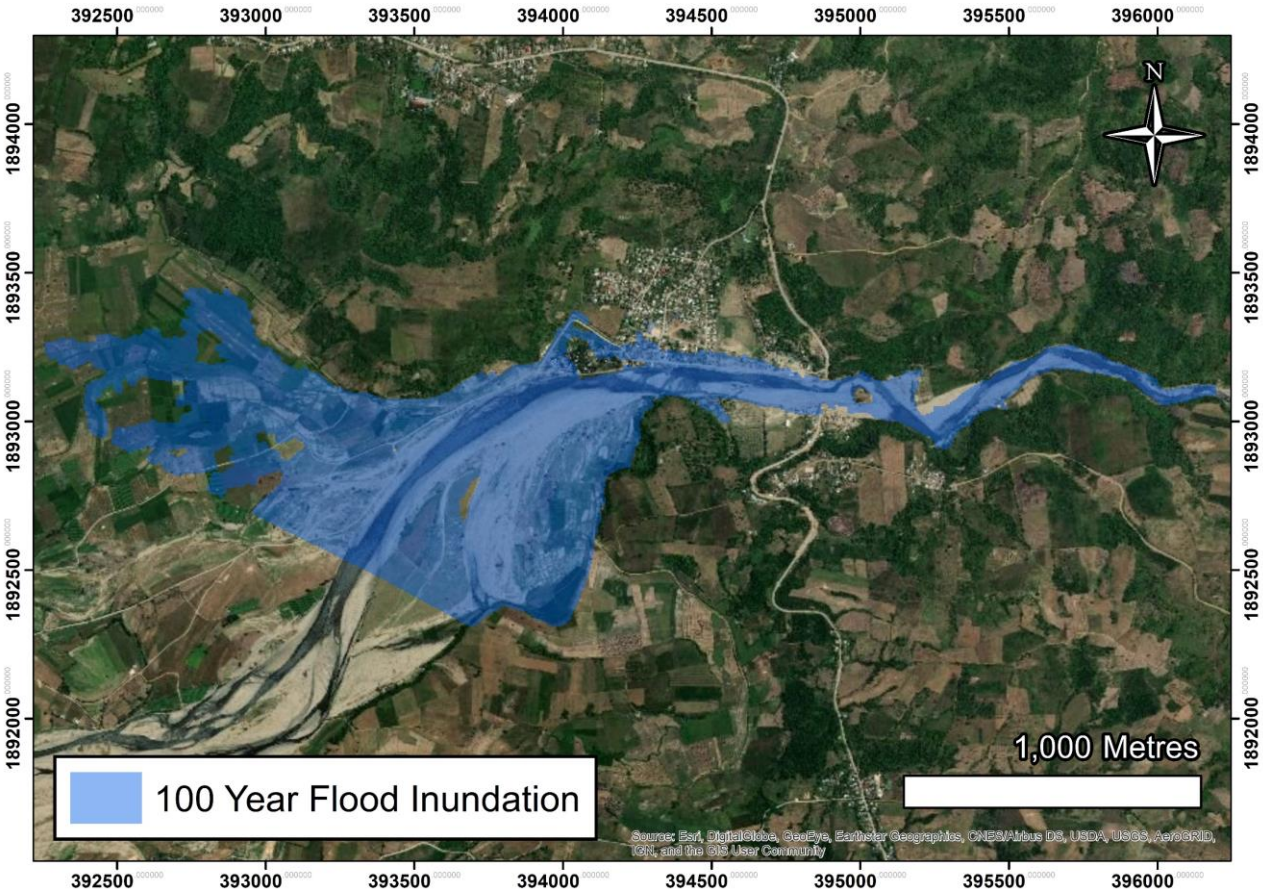

Figure. 5.3.5. *A map showing the total flood inundation in the study area for a flood with a 100-year return period.*

The results for a 100-year return period flood event show a total flood inundation area of 880525m^2 with 89 buildings at risk of flooding (Figure. 5.3.5.).

5.4 Overall Results in Figures

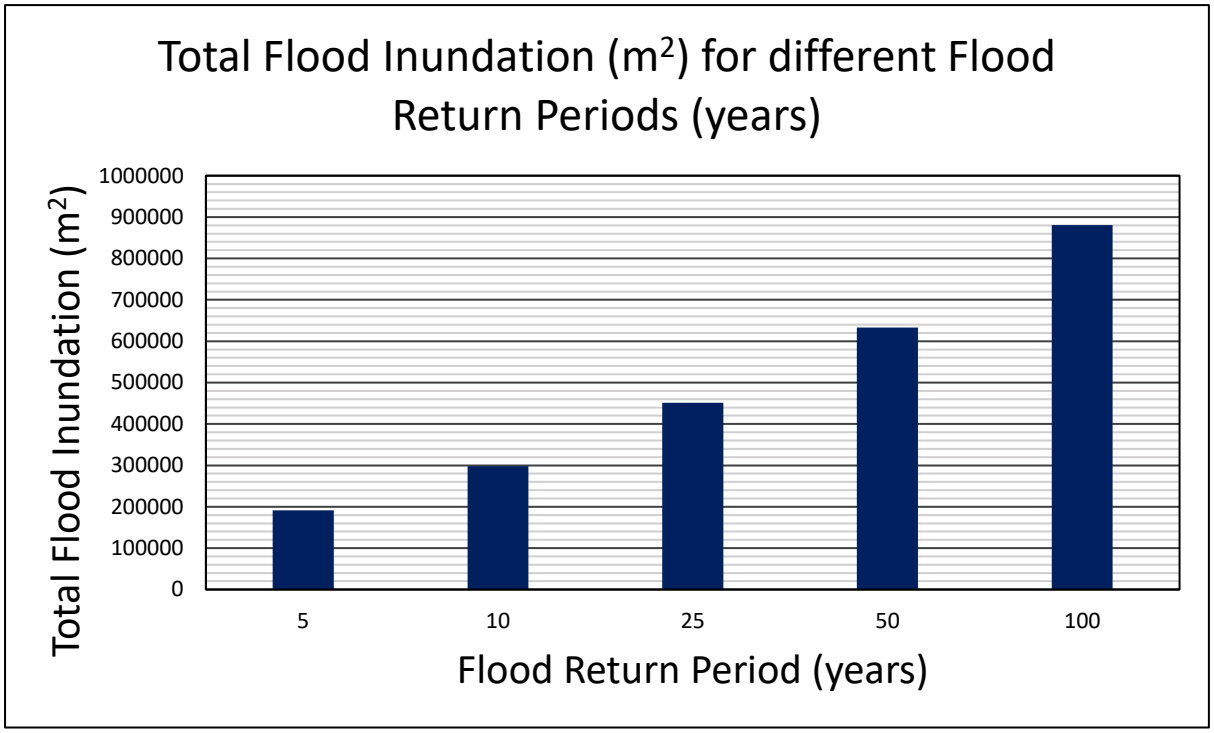

Figure. 5.4.A. *A graph showing the total flood inundation area (m²) for a series of flood events with different return periods. Table 5.4. contains numerical results.*

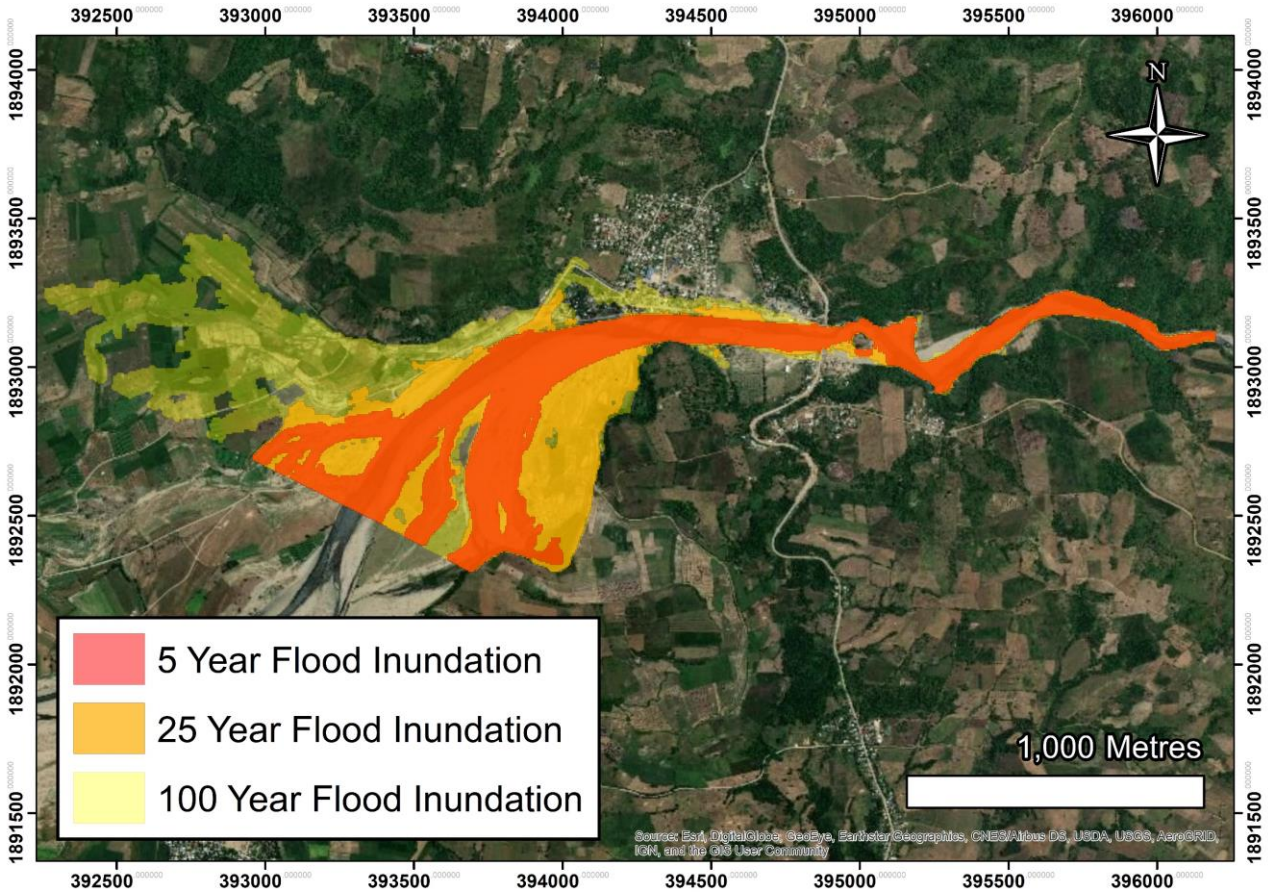

Figure. 5.4.B. *A map showing the total flood inundation in the study area for a 5, 25 and a 100-year flood event for visual comparison. Table 5.4. contains numerical results.*

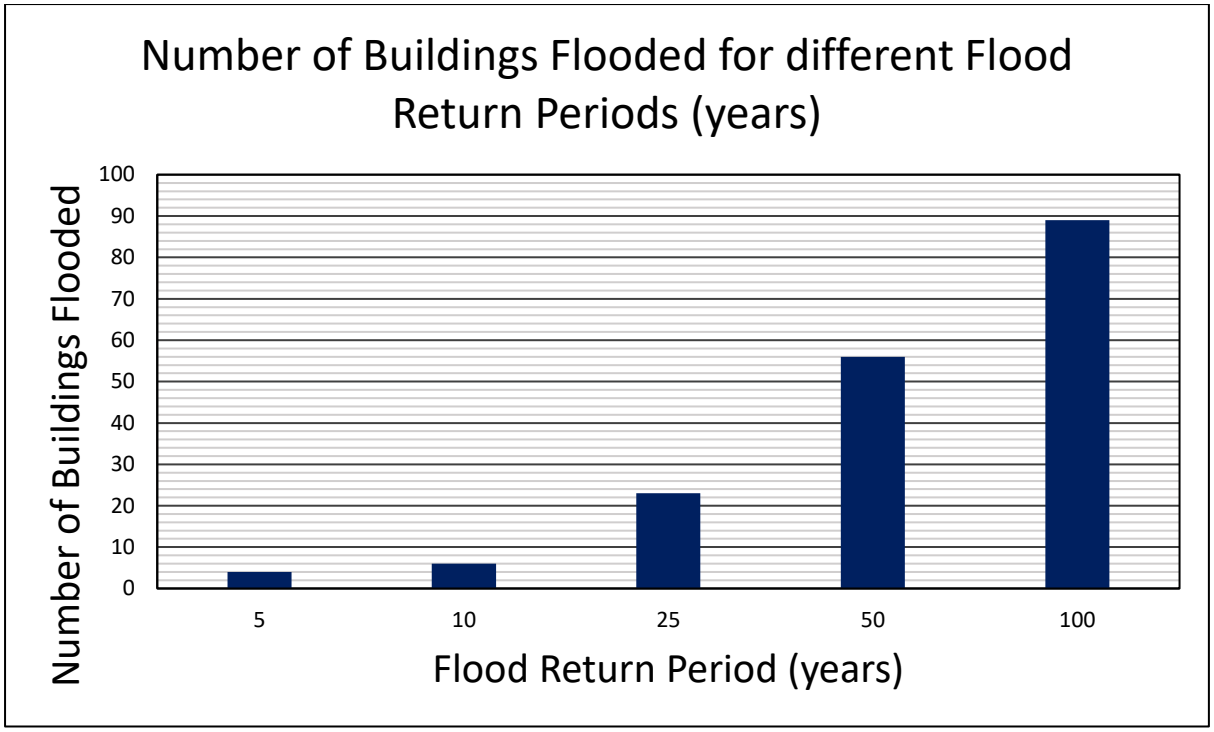

Figure. 5.4.C. *A graph showing the number of buildings flooded in the study area for a series of flood events with different return periods. Table 5.4. contains numerical results.*

Flood Event Return Period (years)	**Total Flood Inundation Area (m^2)**	**Number of Buildings Flooded**
5	191500	4
10	297725	6
25	451525	23
50	632925	56
100	880525	89

Table. 5.4. *A table containing all results for the return period flood event production runs including total flood inundation (m^2) and number of buildings within the inundation area.*

Chapter 6 – Discussion

6.1 Sensitivity Analysis

6.1.1 Floodplain Roughness

The results from the sensitivity analysis undertaken altering floodplain roughness (Figure. 5.1.1.A.)(Figure. 5.1.1.B.) show a trend of increasing inundation area with increasing floodplain roughness between Manning's n values of 0.055 and 0.2. This is consistent with the literature (Apel et al., 2009; Bates et al., 2004; Dung et al., 2011; Hall et al., 2005; Mason et al., 2003; Merwade et al., 2008; Pappenberger et al., 2005; Pappenberger et al., 2007; Pappenberger et al., 2008; Romanowicz & Beven., 2003) and makes sense as higher roughness will slow waters movement through the model, increasing total inundation. However, the results for Manning's n values of <0.055 show a sharp increase in flood inundation with decreasing floodplain roughness, not following a clear trend. This is not consistent with the literature and was analysed further. This was determined to be due to instability in the model with Froude numbers exceeding 1 and supercritical flow taking place due to the reduced roughness allowing faster movement of water (Chanson., 2004; ISIS., 2013). However, given that the estimated roughness values were significantly larger than 0.055 it was not an issue for completing this dissertation.

In percentage terms altering the floodplain roughness had a clear effect on total flood inundation. Therefore, uncertainty in the floodplain roughness could affect results, especially given the subjective nature of the methods used in estimating floodplain roughness. It was observed that the section of the study area that saw the vast majority of increased inundation was in the lower section of the floodplain, with little change in inundation area near Rang-Ayan. Therefore, uncertainty in the floodplain roughness appeared to have a larger effect in the lower, less steep section of the study area and less of an effect in the upper section near Rang-Ayan. As the aim of this dissertation is to assess flood risk (primarily in Rang-Ayan), uncertainty in the floodplain roughness actually plays less of a role than would be expected from the literature (Apel et al., 2009; Bates et al., 2004; Dung et al., 2011; Hall et al., 2005; Mason et al., 2003; Merwade et al., 2008; Pappenberger et al., 2005; Pappenberger et al., 2007; Pappenberger et al., 2008; Romanowicz & Beven., 2003).

6.1.2 Model Timestep

The results from the sensitivity analysis undertaken altering the model timestep (Figure. 5.1.2.) show only little variation in inundation area between timesteps of 0.25s and 2.5s and becomes unstable for timesteps >2.5s. This is consistent with the literature (Courant et al., 1967; Neelz & Pender., 2013; Teng el al., 2017) as the model becomes unstable at timesteps over half of the input DEM resolution (>2.5 for the 5M DEM) due to the Courant-Friedrichs-Lewy stability condition not being satisfied.

In percentage terms altering the model timestep within the stable range had limited effects on total flood inundation. Therefore, the uncertainty relating to the subjective choice of timestep is small and unlikely to have a significant effect on model results. It is therefore optimal to choose a timestep of half of DEM resolution to achieve the lowest possible run times whilst still providing consistent results.

6.1.3 DEM Resolution

The results from the sensitivity analysis undertaken altering the input DEM resolution show a trend of increasing inundation area with increasing grid size of the input DEM (Figure. 5.1.3.). This is consistent with the literature (Bates et al., 1998; Cook & Merwade., 2009; Horritt and Bates, 2001b; Yu and Lane, 2006; Savage et al., 2016a; Savage et al., 2016b) and makes sense for the study area due to its small scale and complex microtopography, which when smoothed out in a coarser DEM could significantly affect results (Dottori et al., 2013; Savage et al., 2016b).

In percentage terms altering the input DEM resolution had a large effect on inundation area. Therefore, the uncertainty relating to the subjective choice of DEM resolution is considerable. In the study area – representative of a small topographically complex tropical upland river – it was determined that of the resolutions tested a 5m DEM was the optimal choice.

6.1.4 Normal Depth Slope

The results from the sensitivity analysis undertaken altering the normal depth slope of the downstream boundary (Figure. 5.1.4.) show a trend of decreasing inundation area with increasing normal depth slope. This makes sense as a steeper downstream boundary would cause water to drain from the model at a faster rate however there is little literature to compare results with. Also 5, 25 and 100-year flood maps produced

for the Ilagan (Paringit & Floresca., 2017) were analysed to assess whether there would be significant backwater effects at the downstream boundary of the study area, depending on if the Ilagan was in high flow. It was determined that given the distance from the confluence of the Bintacan and the Ilagan, that backwater effects would likely not affect model results significantly.

In percentage terms altering the normal depth slope had little effect on inundation area. Therefore, the uncertainty relating to the choice of normal depth slope is relatively small and has little effect on model results.

6.2 Hydrological Sensitivity Analysis

6.2.1 Time to Peak Flow

The results from the hydrological sensitivity analysis undertaken altering the time to peak of the input hydrograph (Figure. 5.2.1.) show little variation in inundation area. This indicates that total volume and peak flow within a set event time control flood inundation, and the shape of the hydrograph within the event has little effect on model results.

In percentage terms the time to peak flow of the input hydrograph had little effect on inundation area. Therefore, the uncertainty relating to the time to peak of the hydrograph for a given volume and event duration is small and is unlikely to have a significant effect on model results. This is useful to know as for the study area – a representative ungauged catchment – estimating the time to peak of input hydrographs proves challenging (Alexander., 1972; Heerdegen., 1974).

6.2.2 Total Event Duration

The results from the hydrological sensitivity analysis undertaken altering the total event duration (keeping total volume of flow constant) (Figure. 5.2.2.) show a trend of decreasing flood inundation as total event duration increases. This is consistent with the literature (Beven et al., 2011; Merz & Thieken., 2005; Pappenberger et al., 2006; Pappenberger et al., 2008; Renard et al., 2010., Savage et al., 2016a) and makes sense as more intense shorter duration high flow events are likely to cause more flooding than longer duration lower intensity events. The results show that for shorter duration events there are larger changes in inundation between events and for longer duration events the changes in inundation between events are significantly less.

In percentage terms the total event duration/intensity had a large effect on inundation area, especially for shorter higher intensity events. Therefore, the uncertainty relating to the high flow event duration and intensity could have a large effect on model results. The uncertainty is greatest for shorter higher intensity events like those experienced during typhoons. Therefore, for the study area – a representative small ungauged upland tropical catchment which experiences frequent typhoons – uncertainty relating to the duration and intensity of high flow events is likely to be the most significant source of uncertainty related to model results, especially given the difficulty of estimating peak flow and volume for an ungauged catchment (Alexander., 1972; Heerdegen., 1974).

6.3 Ranking Sources of Uncertainty Tested

The different sources of uncertainty analysed will now be ranked based upon which sources were determined to have the largest effect on model results (Beven et al., 2015; Dottori et al., 2013; Teng et al., 2017). For the study area – a representative small ungauged topographically complex tropical upland catchment – uncertainty relating to the total event duration and intensity of input hydrology was found to have the largest effect on model results, mostly due to the lack of river gauges and flow data for the Bintacan making estimating peak flow values and event duration challenging. Uncertainty relating to the choice of DEM resolution was found to have the second largest effect on model results likely due to the smoothing out of microtopography at coarser DEM resolutions. Uncertainty relating to the choice of floodplain roughness was found to have the third largest effect on model results, as long as a roughness value within the stable range was chosen, and influences results less than would be expected from the literature. Uncertainty relating to the choice of normal depth slope for the downstream boundary had a small effect on model results and backwater effects were determined to also likely have little effect on model results. Uncertainty relating to the choice of model timestep had little effect on model results, as long as a timestep in the stable range was chosen, and uncertainty relating to the time to peak for the input hydrograph had the least effect on model results.

6.4 Qualitative Analysis of Untested Sources of Uncertainty

Sources of uncertainty not analysed in this dissertation will now be qualitatively assessed. Although not tested, qualitatively the uncertainty associated with the LiDAR,

50cm horizontal accuracy and 20cm vertical accuracy (Paringit & Floresca., 2017), likely had little effect on model results due to the high accuracy of data collection. Qualitatively the change in the river morphology and bathymetry over time could have a significant effect on model results for a tropical river with rapidly changing morphology (Dingle et al., 2019; Pender., 2016; Wong., 2015). Qualitatively the uncertainty associated with the low flow calibration satellite imagery (Stephens et al., 2012) likely had little effect on model results due to the large scale of the high flow events compared to the low flow initial conditions. Even qualitatively it is very difficult to assess the uncertainty related to choice of model structures due to only having used one type of model in this dissertation (Apel et al., 2009; Gupta et al., 2012; Pappenberger et al., 2006; Renard et al., 2010; Willis et al., 2019). Uncertainties related to the change in land use are also difficult to assess even qualitatively (Beven., 2010) and likewise for uncertainty related to changes in climatic conditions (Hirabayashi et al, 2013; Neal et al., 2013).

6.5 Production Runs

6.5.1 5-Year

The results for the 5-year flood showed 4 buildings within the inundation area. Upon inspection of satellite imagery all 4 buildings appear to be sheds or farm buildings as opposed to houses. Before and after satellite imagery for Super Typhoon Lawin was analysed and all 4 buildings were determined to have been destroyed in the subsequent flooding. Therefore, a 5-year flood taking place now would likely pose no risk to any buildings within the study area. Overall there is limited flooding in Rang-Ayan with no houses flooded and a small amount of flooding of agricultural land downstream.

6.5.2 10-Year

The results for the 10-year flood showed 6 buildings within the inundation area. Upon inspection of satellite imagery, the 2 extra buildings flooded also appeared to be farm buildings as opposed to houses. Overall, there is limited flooding in Rang-Ayan with no houses flooded and a slightly larger area of agricultural land flooded downstream compared to the 5-year flood.

6.5.3 25-Year

The results for the 25-year flood showed 23 buildings within the inundation area. Approximately 10 houses within Rang-Ayan were flooded along with many smaller buildings. Upon inspection of before and after satellite imagery, the two areas of the town which were flooded are the same areas were houses were destroyed during super typhoon Lawin (Dingle et al., 2019). This satellite imagery also shows deposition of sediments in the same areas that were predicted to be flooded for the 25-year event. Therefore, it was determined that the flooding caused by super typhoon Lawin was likely equivalent to a 25-year return period flood. Overall, there was a significant increase in flooding within Rang-Ayan with approximately 10 houses flooded and a slightly larger area of agricultural land flooded downstream compared to the 10-year flood.

6.5.4 50-Year

The results for the 50-year flood showed 56 buildings within the inundation area. Upon inspection of satellite imagery, approximately 26 houses within Rang-Ayan were flooded along with many smaller buildings. The area of flooding within Rang-Ayan was over 2.5 times greater than that of the 25-year flood. Overall, there was a large increase in flooding within Rang-Ayan with approximately 26 houses flooded and a larger area of agricultural land flooded downstream compared to the 25-year flood.

6.5.5 100-Year

The results for the 100-year flood showed 89 buildings within the inundation area. Upon inspection of satellite imagery, approximately 47 houses within Rang-Ayan were flooded along with many smaller buildings. The area of flooding within Rang-Ayan was over 2 times greater than that of the 50-year flood. Overall, there was a large increase in flooding within Rang-Ayan with approximately 47 houses flooded and a far larger area of agricultural land flooded downstream compared to the 50-year flood.

6.6 Overall Results – Flood Risk Within the Study Area

The results for the 5, 10, 25, 50 and 100-year events were used to assess flood risk in the area. Overall, the study area was determined to be at high risk of flooding especially from the longer return period events. For both 5 and 10-year events no houses within the study area were found to be at risk of flooding however several sheds and farm

buildings and a small section of agricultural land were found to be at risk. For the 25, 50 and 100-year flood events Rang-Ayan was found to be at risk of considerable flooding, with increasing numbers of houses, smaller buildings and increasing area of agricultural land flooded as the return period of flood events increased. A 100-year flood poses a large risk of destruction of property in Rang-Ayan and would likely cause considerable damage to a large area of agricultural land downstream.

6.7 Representation of Uncertainty with Model Results

The results of this dissertation have all been presented using deterministic flood maps due to the local sensitivity analysis used (Teng et al., 2017). These deterministic flood maps do not communicate the results of uncertainty analysis which is important in flood inundation modelling, as the results could lead to false confidence (Beven et al., 2015; Dottori et al., 2013). This is especially important in the study area as a small movement of the inundation boundary in Rang-Ayan caused a considerable change in the number of buildings flooded, with many buildings very close to the edge of the inundation areas for the return period flood events. Despite probabilistic flood maps being preferable to deterministic flood maps, due to their representation of uncertainty, probabilistic flood mapping was not possible for this dissertation (Bates et al., 2004; Hall et al., 2011; Pappenberger et al., 2005; Romanowicz & Beven., 2003; Teng et al., 2017). This was due to the computationally intensive nature of the model required in the topographically complex study area, with high model run times and a high number of model variables, meaning probabilistic flood mapping would take a prohibitively long time (Afshari., 2018; Neelz & Pender., 2013; Teng et al., 2017). Therefore, it needs to be stressed that the deterministic flood maps produced are not absolutely accurate results and have a number of uncertainties associated with them.

Chapter 7 – Conclusion

The study area looked at was a section of the Bintacan de Ilagan River in the Philippines and was representative of a small ungauged topographically complex tropical upland catchment. For the representative study area, it was determined that a 1D/2D linked hydraulic model was the optimal choice to model flood inundation. Sources of uncertainty were identified including: model variables, model inputs, choice of model structure, changes in floodplain characteristics, changes in river morphology, changes in climatic conditions and uncertainty relating to calibration data. For the representative study area, it was determined that the optimal method for quantifying uncertainty in model results was local sensitivity analysis and deterministic flood mapping was necessitated by the study area. The results from sensitivity analysis found that for the representative study area the uncertainties analysed ranked as follows: uncertainty relating to the intensity/duration for input hydrology, uncertainty relating to the choice of DEM resolution, the choice of floodplain roughness, the choice of normal depth slope of the downstream boundary, the choice of model timestep and uncertainty with the time to peak for the input hydrograph. The results from the return period flood events showed that the study area was at high risk of flooding especially for longer return period events. For both 5 and 10-year flood events no houses in the study area were found to be at risk of flooding however several sheds and farm buildings and a section of agricultural land were found to be at risk. For the 25, 50 and 100-year flood events Rang-Ayan was found to be at risk of considerable flooding, with increasing numbers of houses and smaller buildings flooded and increasing area of agricultural land flooded as the return period of flood events increased. A 100-year flood was found to pose a large risk of destruction of property in Rang-Ayan and would likely cause considerable damage to a large area of agricultural land downstream.

In general, for areas similar to the representative study area in this dissertation it is recommended to use a 1D/2D linked hydraulic model (or at least a 2D model) and local sensitivity analysis. It is also recommended that for areas similar to the representative catchment uncertainties with the input hydrology should be assessed as this can have a large effect on model results. Finally, it is recommended that for similar study areas a careful consideration of input DEM resolution is undertaken as this choice can have a large effect on model results.

Limitations of this dissertation include the lack of high flow model calibration, the lack of validation data to assess model results and the lack of representation of uncertainty in model results. High flow model calibration could not be undertaken due to the lack of flow data for the Bintacan catchment and the lack of satellite imagery to calibrate the model. For the same reasons validation of model results could not be undertaken either making it difficult to assess the accuracy of results. Uncertainty was also not well represented in the deterministic flood maps and it needs to be stressed that the deterministic flood maps are not absolutely accurate results and have a number of uncertainties associated with them.

Given more time, sensitivity analysis could be undertaken altering more than one variable or input at once to assess the relationships between variables while still using somewhat local sensitivity analysis. This would give a better understanding of the uncertainties associated with model results and the relationships between model variables and inputs. Also, sensitivity analysis could be undertaken on each return period flood event to assess whether the ranking of uncertainties differs with the size of the flood event. And finally, sensitivity analysis could be undertaken to assess the ranking of uncertainties throughout a flood event to determine whether the dominant uncertainties change throughout the course of an event.

Despite its limitations this dissertation successfully fills the locational gap in the literature and provides flood risk mapping for an area previously uncovered which is at high risk of damage from flooding.

Appendices

Appendix A – Sensitivity Analysis Results – Floodplain Roughness

Table. 1. *A table containing all results for the sensitivity analysis undertaken altering the floodplain roughness (Manning's n).*

Floodplain Roughness (Manning's n)	Total Flood Inundation Area (m^2)
0.01	376900
0.015	324325
0.02	297250
0.025	291050
0.03	281275
0.035	249250
0.04	245525
0.045	247225
0.05	227650
0.055	166450
0.06	167025
0.07	169075
0.08	171125
0.09	172625
0.1	174200
0.11	175500
0.12	176475
0.13	177750
0.14	178750
0.15	179725
0.16	180525
0.17	181225
0.18	181750
0.19	182225
0.2	182675

Appendix B – Sensitivity Analysis Results – Model Timestep

Table. 2. *A table containing all results for the sensitivity analysis undertaken altering the model timestep (seconds).*

Model Timestep (s)	Total Flood Inundation Area (m^2)
0.25	175900
0.5	176175
0.75	176200
1	176200
1.25	176200
1.5	176300
1.75	176450
2	176475
2.25	176500
2.5	176600
2.75	223600
3	247700
3.25	254250
3.5	259825
3.75	287500
4	293600
4.25	296000
4.5	297325
4.75	299425
5	299625

Appendix C – Sensitivity Analysis Results – DEM Resolution

Table. 3. *A table containing all results for the sensitivity analysis undertaken altering the resolution of the input DEM (m).*

DEM Resolution (m)	Total Flood Inundation Area (m^2)
5	176475
10	188900
15	214425
20	243200
25	253750

Appendix D – Sensitivity Analysis Results – Normal Depth Slope

Table. 4. *A table containing all results for the sensitivity analysis undertaken altering the normal depth slope of the downstream boundary.*

Downstream Boundary Normal Depth Slope	Total Flood Inundation Area (m^2)
0.001	178275
0.001125	177850
0.00125	177475
0.001375	177175
0.0015	176950
0.001625	176775
0.00175	176650
0.001875	176550
0.002	176475
0.002125	176400
0.00225	176325
0.002375	176275
0.0025	176225
0.002625	176175
0.00275	176125
0.002875	176100
0.003	176075

Appendix E – Hydrological Analysis Results – Total Event Duration

Table. 5. *A table containing all results for the hydrological sensitivity analysis undertaken altering the total event duration (hours), keeping total volume of flow constant. i.e. altering the intensity and duration of high flow events.*

Total Event Duration (hours)	Total Flood Inundation Area (m^2)
3	1198675
4	678775
5	472975
6	386225
7	293800
8	228750
9	197025
10	176475
11	161625
12	147050
13	132250
14	119275
15	106225
16	93575
17	85425
18	78075
19	68200
20	56900
21	46925
22	43225
23	41000
24	39975

Appendix F – Hydrological Analysis Results – Time to Peak Flow

Table. 6. *A table containing all results for the hydrological sensitivity analysis undertaken altering the time to peak for the input hydrograph (hours), keeping total volume of flow constant.*

Time to Peak for the Input Hydrograph (Hours)	**Total Flood Inundation Area (m^2)**
0.5	176850
0.75	176800
1	176750
1.25	176725
1.5	176700
1.75	176700
2	176650
2.225	176650
2.5	176625
2.75	176600
3	176575
3.25	176575
3.5	176550
3.75	176550
4	176525
4.25	176500
4.5	176500
4.75	176475
5	176475

Appendix G – Return Period Flood Event Results – Total Flood Inundation

Table. 7. *A table containing all results for the return period flood event production runs including total flood inundation (m^2) and number of buildings within the inundation area.*

Flood Event Return Period (years)	Total Flood Inundation Area (m^2)	Number of Buildings Flooded
5	191500	4
10	297725	6
25	451525	23
50	632925	56
100	880525	89

References

Abily, M., Bertrand, N., Delestre, O., Gourbesville, P. and Duluc, C.M., 2016. Spatial Global Sensitivity Analysis of High Resolution classified topographic data use in 2D urban flood modelling. Environmental Modelling & Software, 77, pp.183-195.

Afshari, S., Tavakoly, A.A., Rajib, M.A., Zheng, X., Follum, M.L., Omranian, E. & Fekete, B.M. 2018, "Comparison of new generation low-complexity flood inundation mapping tools with a hydrodynamic model", Journal of Hydrology, vol. 556, pp. 539-556.

Ahmadisharaf, E., Kalyanapu, A.J. & Bates, P.D. 2018, "A probabilistic framework for floodplain mapping using hydrological modeling and unsteady hydraulic modeling", Hydrological Sciences Journal, vol. 63, no. 12, pp. 1759-1775.

Alexander, G.N. 1972, "Effect of catchment area on flood magnitude", Journal of Hydrology, vol. 16, no. 3, pp. 225-240.

Alfieri, L., Bisselink, B., Dottori, F., Naumann, G., Roo, A., Salamon, P., Wyser, K. & Feyen, L. 2017, "Global projections of river flood risk in a warmer world", Earth's Future, vol. 5, no. 2, pp. 171-182.

Apel, H., Aronica, G.T., Kreibich, H. and Thieken, A.H., 2009. Flood risk analyses—how detailed do we need to be?. Natural Hazards, 49(1), pp.79-98.

Arcement, G.J. and Schneider, V.R., 1989. Guide for selecting Manning's roughness coefficients for natural channels and flood plains.

Archer, L., Neal, J.C., Bates, P.D. & House, J.I. 2018, "Comparing TanDEM-X Data With Frequently Used DEMs for Flood Inundation Modeling", Water Resources Research, vol. 54, no. 12, pp. 10,205-10,222.

Arnell, N.W., & Gosling, S.N. 2016, "The impacts of climate change on river flood risk at the global scale", Climatic Change, vol. 134, no. 3, pp. 387-401.

Balderama, O. F., Alejo, L. A., Tongson, E., Rhia, E., Pantola, T., 2017, Development and Application of Corn Model for climate Change Impact Assessment and Decision support System: Enabling Philippine Farmers Adapt to climate Variability in: Walter Leal Filho (Eds.), climate Change Research at universities, 373-387.

Balica, S.F., Popescu, I., Beevers, L. and Wright, N.G., 2013. Parametric and physically based modelling techniques for flood risk and vulnerability assessment: a comparison. Environmental modelling & software, 41, pp.84-92.

Bates P.D., Anderson, M.G. 1993, A two-dimensional finite-element model for river flow inundation. Proceedings of the Royal Society of London, Series A: Mathematical, Physical and Engineering Sciences 440: 481–491.

Bates, P.D. & De Roo, A.P.J. 2000, "A simple raster-based model for flood inundation simulation", Journal of Hydrology, vol. 236, no. 1, pp. 54-77.

Bates, P.D. 2012, "Integrating remote sensing data with flood inundation models: how far have we got?", Hydrological Processes, vol. 26, no. 16, pp. 2515-2521.

Bates, P.D., Horritt, M. and Hervouet, J.M., 1998. Investigating two-dimensional, finite element predictions of floodplain inundation using fractal generated topography. Hydrological processes, 12(8), pp.1257-1277.

Bates, P.D., Horritt, M.S., Aronica, G. and Beven, K., 2004. Bayesian updating of flood inundation likelihoods conditioned on flood extent data. Hydrological Processes, 18(17), pp.3347-3370.

Beven, K., 2011. 14 Distributed Models and Uncertainty in Flood Risk Management. Flood risk science and management, p.291.

Beven, K., Lamb, R., Leedal, D. and Hunter, N., 2015. Communicating uncertainty in flood inundation mapping: a case study. International Journal of River Basin Management, 13(3), pp.285-295.

Beven, K., Leedal, D., McCarthy, S., Lamb, R., Hunter, N., Keef, C., Bates, P., Neal, J. and Wicks, J., 2011. Framework for assessing uncertainty in fluvial flood risk mapping. FRMRC Research Rep. SWP1, 7.

Bradbrook, K.F., Lane, S.N., Waller, S.G. & Bates, P.D. 2004, "Two dimensional diffusion wave modelling of flood inundation using a simplified channel representation", International Journal of River Basin Management, vol. 2, no. 3, pp. 211-223.

Brunner, G.W. 2016, HEC-RES River Analysis System - User's Manual Version 5.0. US Army Corps of Engineers, Institute for Water Resources, Hydrologic Engineering Center, pp. 962.

Casulli, V. and Stelling, G.S., 1998. Numerical simulation of 3D quasi-hydrostatic, free-surface flows. Journal of Hydraulic Engineering, 124(7), pp.678-686.

Census of Population. 2015. Highlights of the Philippine Population 2015 Census of Population. PSA.

Chanson, H., 2004. Hydraulics of open channel flow. Elsevier.

Chow, V.T., 1959. Open channel flow. London: McGRAW-HILL, 11(95), pp.99-136.

Cleary, P.W. and Prakash, M., 2004. Discrete–element modelling and smoothed particle hydrodynamics: potential in the environmental sciences. Philosophical Transactions of the Royal Society of London. Series A: Mathematical, Physical and Engineering Sciences, 362(1822), pp.2003-2030.

Cobby, D.M., Mason, D.C. and Davenport, I.J., 2001. Image processing of airborne scanning laser altimetry data for improved river flood modelling. ISPRS Journal of Photogrammetry and Remote Sensing, 56(2), pp.121-138.

Cobby, D.M., Mason, D.C., Horritt, M.S. and Bates, P.D., 2003. Two-dimensional hydraulic flood modelling using a finite-element mesh decomposed according to vegetation and topographic features derived from airborne scanning laser altimetry. Hydrological processes, 17(10), pp.1979-2000.

Cook, A. & Merwade, V. 2009, "Effect of topographic data, geometric configuration and modeling approach on flood inundation mapping", Journal of Hydrology, vol. 377, no. 1, pp. 131-142.

Costabile, P., Macchione, F., Natale, L. and Petaccia, G., 2015. Flood mapping using LIDAR DEM. Limitations of the 1-D modeling highlighted by the 2-D approach. Natural Hazards, 77(1), pp.181-204.

Courant, R., Friedrichs, K. and Lewy, H., 1967. On the partial difference equations of mathematical physics. IBM journal of Research and Development, 11(2), pp.215-234.

del Rosario, E.D., 2014, FINAL REPORT Effects of Typhoon YOLANDA (HAIYAN). NDRRMC.

DHI. 2003, MIKE 11-A Modelling System for Rivers and Channels - User Guide DHI, pp. 430.

DHI. 2012, MIKE 21-2D Modelling of Coast and Sea, DHI Water & Environment Pty Ltd.

Dingle, E.H., Paringit, E.C., Tolentino, P.L., Williams, R.D., Hoey, T.B., Barrett, B., Long, H., Smiley, C. & Stott, E. 2019, "Decadal-scale morphological adjustment of a lowland tropical river", Geomorphology, vol. 333, pp. 30-42.

Dottori, F., Di Baldassarre, G. & Todini, E. 2013, "Detailed data is welcome, but with a pinch of salt: Accuracy, precision, and uncertainty in flood inundation modeling", Water Resources Research, vol. 49, no. 9, pp. 6079-6085.

Dung, N.V., Merz, B., Bárdossy, A., Thang, T.D. and Apel, H., 2011. Multi-objective automatic calibration of hydrodynamic models utilizing inundation maps and gauge data. Hydrology and Earth System Sciences, 15(4), pp.1339-1354.

Ernst, J., Dewals, B.J., Detrembleur, S., Archambeau, P., Erpicum, S. and Pirotton, M., 2010. Micro-scale flood risk analysis based on detailed 2D hydraulic modelling and high resolution geographic data. Natural Hazards, 55(2), pp.181-209.

Fewtrell, T.J., Duncan, A., Sampson, C.C., Neal, J.C. and Bates, P.D., 2011. Benchmarking urban flood models of varying complexity and scale using high resolution terrestrial LiDAR data. Physics and Chemistry of the Earth, Parts A/B/C, 36(7-8), pp.281-291.

Gómez, M., Macchione, F. and Russo, B., 2011. Methodologies to study the surface hydraulic behaviour of urban catchments during storm events. Water science and technology, 63(11), pp.2666-2673.

Gomez-Valentin, M., Macchione, F. and Russo, B., 2009. Hydraulic behavior of urban streets during storm events. Ingenieria Hidraulica en Mexico, 24(3), pp.51-62.

Guinot, V., 2012. Multiple porosity shallow water models for macroscopic modelling of urban floods. Advances in Water Resources, 37, pp.40-72.

Gupta, H.V., Clark, M.P., Vrugt, J.A., Abramowitz, G. and Ye, M., 2012. Towards a comprehensive assessment of model structural adequacy. Water Resources Research, 48(8).

Hall, J.W., Manning, L.J. and Hankin, R.K., 2011. Bayesian calibration of a flood inundation model using spatial data. Water Resources Research, 47(5).

Hall, J.W., Tarantola, S., Bates, P.D. and Horritt, M.S., 2005. Distributed sensitivity analysis of flood inundation model calibration. Journal of Hydraulic Engineering, 131(2), pp.117-126.

Hedman, E.R. and Osterkamp, W.R., 1982. Streamflow characteristics related to channel geometry of streams in western United States (No. 2193). USGPO.

Heerdegen, R.G. & Reich, B.M. 1974, "Unit hydrographs for catchments of different sizes and dissimilar regions", Journal of Hydrology, vol. 22, no. 1, pp. 143-153.

Hirabayashi, Y., Mahendran, R., Koirala, S., Konoshima, L., Yamazaki, D., Watanabe, S., Kim, H. & Kanae, S. 2013, "Global flood risk under climate change", Nature Climate Change, vol. 3, no. 9, pp. 816-821.

Horritt, M.S. & Bates, P.D. 2002, "Evaluation of 1D and 2D numerical models for predicting river flood inundation", Journal of Hydrology, vol. 268, no. 1, pp. 87-99.

Horritt, M.S. 2006, "A methodology for the validation of uncertain flood inundation models", Journal of Hydrology, vol. 326, no. 1, pp. 153-165.

Horritt, M.S. and Bates, P.D., 2001a. Predicting floodplain inundation: raster-based modelling versus the finite-element approach. Hydrological processes, 15(5), pp.825-842.

Horritt, M.S. and Bates, P.D., 2001b. Effects of spatial resolution on a raster based model of flood flow. Journal of Hydrology, 253(1-4), pp.239-249.

Horritt, M.S., Bates, P.D. and Mattinson, M.J., 2006. Effects of mesh resolution and topographic representation in 2D finite volume models of shallow water fluvial flow. Journal of Hydrology, 329(1-2), pp.306-314.

Hunter, N.M., Bates, P.D., Neelz, S., Pender, G., Villanueva, I., Wright, N.G., Liang, D., Falconer, R.A., Lin, B., Waller, S. and Crossley, A.J., 2008, February. Benchmarking 2D

hydraulic models for urban flooding. In Proceedings of the Institution of Civil Engineers-Water Management (Vol. 161, No. 1, pp. 13-30). Thomas Telford Ltd.

ISIS. 2013. ISIS 2D Quick Start Guide.
https://www.floodmodeller.com/media/34732/isis_2d_quick_start_guide.pdf

Jacobs. 2019, Flood Modeller Online Guide,
http://help.floodmodeller.com/floodmodeller/

Jalad, R.B. 2018, Situational Report No.55 re Preparedness Measures for TY OMPONG (I.N. MANGKHUT). NDRRMC.

Jonkman, S.N., Vrijling, J.K. and Vrouwenvelder, A.C.W.M., 2008. Methods for the estimation of loss of life due to floods: a literature review and a proposal for a new method. Natural Hazards, 46(3), pp.353-389.

Kimutai, K. 2018, "Longest Rivers In The Philippines". worldatlas.com. WorldAtlas.

Kron, W. 2005, "Flood Risk = Hazard Values Vulnerability", Water International, vol. 30, no. 1, pp. 58-68.

Lhomme, J., Sayers, P.B., Gouldby, B.P., Samuels, P.G., Wills, M. and Mulet-Marti, J., 2008. Recent development and application of a rapid flood spreading method.

Marks, K. and Bates, P., 2000. Integration of high-resolution topographic data with floodplain flow models. Hydrological Processes, 14(11-12), pp.2109-2122.

Mason, D.C., Cobby, D.M., Horritt, M.S. and Bates, P.D., 2003. Floodplain friction parameterization in two-dimensional river flood models using vegetation heights derived from airborne scanning laser altimetry. Hydrological processes, 17(9), pp.1711-1732.

McGrath, H., Bourgon, J., Proulx-Bourque, J., Nastev, M. & Abo El Ezz, A. 2018, "A comparison of simplified conceptual models for rapid web-based flood inundation mapping", Natural Hazards, vol. 93, no. 2, pp. 905-920.

Merriam-Webster., 2019, “Flood.” The Merriam-Webster.com Dictionary, Merriam-Webster Inc., https://www.merriam-webster.com/dictionary/flood.

Merz, B. and Thieken, A.H., 2005. Separating natural and epistemic uncertainty in flood frequency analysis. Journal of Hydrology, 309(1-4), pp.114-132.

Mignot, E., Paquier, A. and Haider, S., 2006. Modeling floods in a dense urban area using 2D shallow water equations. Journal of Hydrology, 327(1-2), pp.186-199.

Moel, H.D., Alphen, J.V. and Aerts, J.C.J.H., 2009. Flood maps in Europe-methods, availability and use.

Monaghan, J.J., 1994. Simulating free surface flows with SPH. Journal of computational physics, 110(2), pp.399-406.

Neal, J., Keef, C., Bates, P., Beven, K. and Leedal, D., 2013. Probabilistic flood risk mapping including spatial dependence. Hydrological Processes, 27(9), pp.1349-1363.

Neal, J., Schumann, G., Fewtrell, T., Budimir, M., Bates, P. and Mason, D., 2011. Evaluating a new LISFLOOD-FP formulation with data from the summer 2007 floods in Tewkesbury, UK. Journal of Flood Risk Management, 4(2), pp.88-95.

Néelz, S. and Pender, G., 2010. Benchmarking of 2D hydraulic modelling packages.

Néelz, S. and Pender, G., 2013. Benchmarking the latest generation of 2D hydraulic modelling packages. Environment Agency, Horison House, Deanery Road, Bristol, BS1 9AH.

Néelz, S., 2009. Desktop review of 2D hydraulic modelling packages. Bristol: Environment Agency.

Nobre, A.D., Cuartas, L.A., Hodnett, M., Rennó, C.D., Rodrigues, G., Silveira, A., Waterloo, M. and Saleska, S., 2011. Height Above the Nearest Drainage–a hydrologically relevant new terrain model. Journal of Hydrology, 404(1-2), pp.13-29.

Organisation for Economic Co-operation and Development (OECD). 2016, Financial Management of Flood Risk, OECD Publishing, Paris.

Paiva, R.C.D., Buarque, D.C., Collischonn, W., Bonnet, M., Frappart, F., Calmant, S. & Bulhões Mendes, C.A. 2013a, "Large-scale hydrologic and hydrodynamic modeling of the Amazon River basin", Water Resources Research, vol. 49, no. 3, pp. 1226-1243.

Paiva, R.C.D., Collischonn, W., Bonnet, M.-., de GonÃ§alves, L. G. G, Calmant, S., Getirana, A. & Santos da Silva, J. 2013b, "Assimilating in situ and radar altimetry data into a large-scale hydrologic-hydrodynamic model for streamflow forecast in the Amazon", Hydrology and Earth System Sciences, vol. 17, no. 7, pp. 2929-2946.

Pappenberger, F., Beven, K., Horritt, M. and Blazkova, S., 2005. Uncertainty in the calibration of effective roughness parameters in HEC-RAS using inundation and downstream level observations. Journal of Hydrology, 302(1-4), pp.46-69.

Pappenberger, F., Beven, K.J., Ratto, M. and Matgen, P., 2008. Multi-method global sensitivity analysis of flood inundation models. Advances in water resources, 31(1), pp.1-14.

Pappenberger, F., Frodsham, K., Beven, K., Romanowicz, R., Matgen, P. 2007, "Fuzzy set approach to calibrating distributed flood inundation models using remote sensing observations", Hydrology and Earth System Sciences, vol. 11, no. 2, pp. 739-752.

Pappenberger, F., Matgen, P., Beven, K.J., Henry, J.B. and Pfister, L., 2006. Influence of uncertain boundary conditions and model structure on flood inundation predictions. Advances in water resources, 29(10), pp.1430-1449.

Paringit, E., and Floresca, J., 2017, LiDAR Surveys and Flood Mapping Report of Pinacanauan de Ilagan River, in Enrico C. Paringit, (Ed.), Flood Hazard Mapping of the Philippines using LIDAR, Quezon City: University of the Philippines Training Center for Applied Geodesy and Photogrammetry – 371pp.

Pelletier, P.M. 1988, "Uncertainties in the single determination of river discharge: a literature review", Canadian Journal of Civil Engineering, vol. 15, no. 5, pp. 834-850.

Prakash, M., Rothauge, K. and Cleary, P.W., 2014. Modelling the impact of dam failure scenarios on flood inundation using SPH. Applied Mathematical Modelling, 38(23), pp.5515-5534.

Qi, H. and Altinakar, M.S., 2011. A GIS-based decision support system for integrated flood management under uncertainty with two dimensional numerical simulations. Environmental Modelling & Software, 26(6), pp.817-821.

Ramos, B.T. 2014, FINAL REPORT re Effects of Typhoon Glenda. NDRRMC.

Renard, B., Kavetski, D., Kuczera, G., Thyer, M. and Franks, S.W., 2010. Understanding predictive uncertainty in hydrologic modeling: The challenge of identifying input and structural errors. Water Resources Research, 46(5).

Richardson, K., Steffen, W. & Liverman, D. 2011, Climate Change: Global Risks, Challenges and Decisions, Cambridge University Press, Cambridge.

Roberts, S., Nielsen, O., Gray, D., Sexton, J. and Davies, G., 2010. ANUGA user manual. Geoscience Australia.

Romanowicz, R. and Beven, K., 2003. Estimation of flood inundation probabilities as conditioned on event inundation maps. Water Resources Research, 39(3).

Russo, B., Gómez, M. and Macchione, F., 2013. Pedestrian hazard criteria for flooded urban areas. Natural hazards, 69(1), pp.251-265.

Samuels, P.G. 1990, Cross section location in one-dimensional models. In International Conference on River Flood Hydraulics, Wiley: Chichester; 339–350.

Savage, J.T.S., Bates, P., Freer, J., Neal, J. and Aronica, G., 2016b. When does spatial resolution become spurious in probabilistic flood inundation predictions?. Hydrological Processes, 30(13), pp.2014-2032.

Savage, J.T.S., Pianosi, F., Bates, P., Freer, J. & Wagener, T. 2016a, "Quantifying the importance of spatial resolution and other factors through global sensitivity analysis of a flood inundation model", Water Resources Research, vol. 52, no. 11, pp. 9146-9163.

Schubert, J.E., Sanders, B.F., Smith, M.J. and Wright, N.G., 2008. Unstructured mesh generation and landcover-based resistance for hydrodynamic modeling of urban flooding. Advances in Water Resources, 31(12), pp.1603-1621.

Schumann, G., Bates, P.D., Horritt, M.S., Matgen, P. & Pappenberger, F. 2009, "Progress in integration of remote sensing–derived flood extent and stage data and hydraulic models", Reviews of Geophysics, vol. 47, no. 4, pp. n/a.

Schumann, G., Matgen, P., Hoffmann, L., Hostache, R., Pappenberger, F. & Pfister, L. 2007, "Deriving distributed roughness values from satellite radar data for flood inundation modelling", Journal of Hydrology, vol. 344, no. 1, pp. 96-111.

Schumann, G.J.-. & Moller, D.K. 2015, "Microwave remote sensing of flood inundation", Physics and Chemistry of the Earth, vol. 83-84, pp. 84-95.

Singh, V. & Goyal, M.K. 2017, "Unsteady High Velocity Flood Flows and the Development of Rating Curves in a Himalayan Basin under Climate Change Scenarios", Journal of Hydrologic Engineering, vol. 22, no. 8, pp. 4017023.

Skinner, C.J., Coulthard, T.J., Parsons, D.R., Ramirez, J.A., Mullen, L. & Manson, S. 2015, "Simulating tidal and storm surge hydraulics with a simple 2D inertia based model, in the Humber Estuary, U.K", Estuarine, Coastal and Shelf Science, vol. 155, pp. 126-136.

Smith, L.C. 1997, "Satellite remote sensing of river inundation area, stage, and discharge: a review", Hydrological Processes, vol. 11, no. 10, pp. 1427-1439.

Soares-Frazão, S., Lhomme, J., Guinot, V. and Zech, Y., 2008. Two-dimensional shallow-water model with porosity for urban flood modelling. Journal of Hydraulic Research, 46(1), pp.45-64.

Stephens, E. and Bates, P., 2015. Assessing the reliability of probabilistic flood inundation model predictions. Hydrological Processes, 29(19), pp.4264-4283.

Stephens, E.M., Bates, P.D., Freer, J.E. and Mason, D.C., 2012. The impact of uncertainty in satellite data on the assessment of flood inundation models. Journal of Hydrology, 414, pp.162-173.

Sun, W., Ishidaira, H., Bastola, S. & Yu, J. 2015, "Estimating daily time series of streamflow using hydrological model calibrated based on satellite observations of river water surface width: Toward real world applications", Environmental Research, vol. 139, pp. 36-45.

Tayefi, V., Lane, S.N., Hardy, R.J. and Yu, D., 2007. A comparison of one-and two-dimensional approaches to modelling flood inundation over complex upland floodplains. Hydrological Processes: An International Journal, 21(23), pp.3190-3202.

Teng, J., Jakeman, A.J., Vaze, J., Croke, B.F.W., Dutta, D. & Kim, S. 2017, "Flood inundation modelling: A review of methods, recent advances and uncertainty analysis", Environmental Modelling and Software, vol. 90, pp. 201-216.

Thome, C.R. & Zevenbergen, L.W. 1985, "Estimating Mean Velocity in Mountain Rivers", Journal of Hydraulic Engineering, vol. 111, no. 4, pp. 612-624.

Tolentino, P.L.M., Poortinga, A., Kanamaru, H., Keesstra, S., Maroulis, J., David, C.P.C. & Ritsema, C.J. 2016, "Projected impact of climate change on hydrological regimes in the Philippines", PLoS ONE, vol. 11, no. 10, pp. e0163941.

UN. 2013a, Global Assessment Report on Disaster Risk Reduction. https://www.unisdr.org/we/inform/publications/33013

UN. 2013b, "Typhoon Haiyan - RW Updates". United Nations Office for the Coordination of Humanitarian Affairs. Philippines: Hundreds of corpses unburied after Philippine typhoon.

UN. 2015, The Human Cost of Weather Related Disasters 1995-2015. https://www.unisdr.org/we/inform/publications/46796

UN. 2016. "Islands of Philippines". Island Directory Tables. United Nations Environment Programme.

Vacondio, R., Rogers, B.D., Stansby, P.K. and Mignosa, P., 2011. SPH modeling of shallow flow with open boundaries for practical flood simulation. Journal of Hydraulic Engineering, 138(6), pp.530-541.

Vora, A., Sharma, P.J., Loliyana, V.D., Patel, P.L. & Timbadiya, P.V. 2018, "Assessment and Prioritization of Flood Protection Levees along the Lower Tapi River, India", Natural Hazards Review, vol. 19, no. 4, pp. 5018009.

Warmink, J.J., Janssen, J.A.E.B., Booij, M.J. and Krol, M.S., 2010. Identification and classification of uncertainties in the application of environmental models. Environmental modelling & software, 25(12), pp.1518-1527.

Willis, T., Wright, N. & Sleigh, A. 2019, "Systematic analysis of uncertainty in 2D flood inundation models", Environmental Modelling & Software, vol. 122, pp. 104520.

Xia, J., Falconer, R.A., Lin, B. and Tan, G., 2011. Numerical assessment of flood hazard risk to people and vehicles in flash floods. Environmental Modelling & Software, 26(8), pp.987-998.

Ye, J. and McCorquodale, J.A., 1998. Simulation of curved open channel flows by 3D hydrodynamic model. Journal of Hydraulic Engineering, 124(7), pp.687-698.

Yu, D. and Lane, S.N., 2006. Urban fluvial flood modelling using a two-dimensional diffusion-wave treatment, part 1: mesh resolution effects. Hydrological Processes: An International Journal, 20(7), pp.1541-1565.

Zischg, A.P., Mosimann, M., Bernet, D.B. & Röthlisberger, V. 2018, "Validation of 2D flood models with insurance claims", Journal of Hydrology, vol. 557, pp. 350-361.